Published July 13, 2015

Donor colonic CD103$^+$ dendritic cells determine the severity of acute graft-versus-host disease

Motoko Koyama,[1] Melody Cheong,[1] Kate A. Markey,[1] Kate H. Gartlan,[1] Rachel D. Kuns,[1] Kelly R. Locke,[1] Katie E. Lineburg,[1] Bianca E. Teal,[1] Lucie Leveque-El mouttie,[1] Mark D. Bunting,[1] Slavica Vuckovic,[1] Ping Zhang,[1] Michele W.L. Teng,[1] Antiopi Varelias,[1] Siok-Keen Tey,[1,4] Leesa F. Wockner,[1] Christian R. Engwerda,[1] Mark J. Smyth,[1] Gabrielle T. Belz,[2] Shaun R. McColl,[3] Kelli P.A. MacDonald,[1] and Geoffrey R. Hill[1,4]

[1]QIMR Berghofer Medical Research Institute, Brisbane, Queensland 4006, Australia
[2]Walter and Eliza Hall Institute of Medical Research, Melbourne, Victoria 3052, Australia
[3]The University of Adelaide, Adelaide, South Australia 5005, Australia
[4]The Royal Brisbane and Women's Hospital, Brisbane, Queensland 4029, Australia

The primacy of the gastrointestinal (GI) tract in dictating the outcome of graft-versus-host disease (GVHD) is broadly accepted; however, the mechanisms controlling this effect are poorly understood. Here, we demonstrate that GVHD markedly enhances alloantigen presentation within the mesenteric lymph nodes (mLNs), mediated by donor CD103$^+$CD11b$^-$ dendritic cells (DCs) that migrate from the colon under the influence of CCR7. Expansion and differentiation of donor T cells specifically within the mLNs is driven by profound levels of alloantigen, IL-12, and IL-6 promoted by Toll-like receptor (TLR) and receptor for advanced glycation end products (RAGE) signals. Critically, alloantigen presentation in the mLNs imprints gut-homing integrin signatures on donor T cells, leading to their emigration into the GI tract where they mediate fulminant disease. These data identify a critical, anatomically distinct, donor DC subset that amplifies GVHD. We thus highlight multiple therapeutic targets and the ability of GVHD, once initiated by recipient antigen-presenting cells, to generate a profound, localized, and lethal feed-forward cascade of donor DC–mediated indirect alloantigen presentation and cytokine secretion within the GI tract.

CORRESPONDENCE
Motoko Koyama:
Motoko.Koyama@qimrberghofer.edu.au
OR
Geoffrey R. Hill:
Geoff.Hill@qimrberghofer.edu.au

Abbreviations used: BLI, bioluminescence imaging; BMT, BM transplant; DAMP, damage-associated molecular pattern; DT, diphtheria toxin; DTR, DT receptor; FLC, fetal liver chimera; GI, gastrointestinal; GVHD, graft-versus-host disease; iLN, inguinal LN; mLN, mesenteric LN; PAMP, pathogen-associated molecular pattern; pLN, peripheral LN; RAGE, receptor for advanced glycation end products; TRIF, Toll–IL-1 receptor domain–containing adaptor inducing IFN-β.

Allogeneic hematopoietic stem cell transplantation is a therapy for hematopoietic malignancies in which cure is achieved by immune-mediated graft-versus-leukemia (GVL) effects. Graft-versus-host disease (GVHD) is a similar process whereby normal tissue, particularly that in gastrointestinal (GI) tract, skin, and liver, is targeted and represents the major limitation of this therapy (Ferrara et al., 2009; Gooley et al., 2010; Weisdorf et al., 2012). Host alloantigens, derived from polymorphic proteins, can be presented to donor T cells by host APCs (direct presentation) or by donor APCs after uptake of cellular material from damaged host target tissue (indirect presentation; Chakraverty and Sykes, 2007; Joffre et al., 2012). In MHC class I–dependent GVHD, host hematopoietic APCs have been shown to be critical for disease, and donor APCs can amplify this effect (Shlomchik et al., 1999; Matte et al., 2004). Recently, we have shown that MHC class II–dependent GVHD may be initiated by nonhematopoietic APCs and donor hematopoietic APCs in isolation are inefficient in initiating disease (MacDonald et al., 2007; Markey et al., 2009; Koyama et al., 2012; Toubai et al., 2012). However, the relative importance of donor indirect alloantigen presentation to GVHD and the cellular and molecular contexts involved have not been established in clinically relevant systems where GVHD has been initiated by recipient antigen presentation. Given that donor APCs are essential to provide pathogen-specific immune

The Rockefeller University Press $30.00
J. Exp. Med. 2015 Vol. 212 No. 8 1303–1321
www.jem.org/cgi/doi/10.1084/jem.20150329

Supplemental Material can be found at:
http://jem.rupress.org/content/suppl/2015/07/08/jem.20150329.DC1.html

Published July 13, 2015

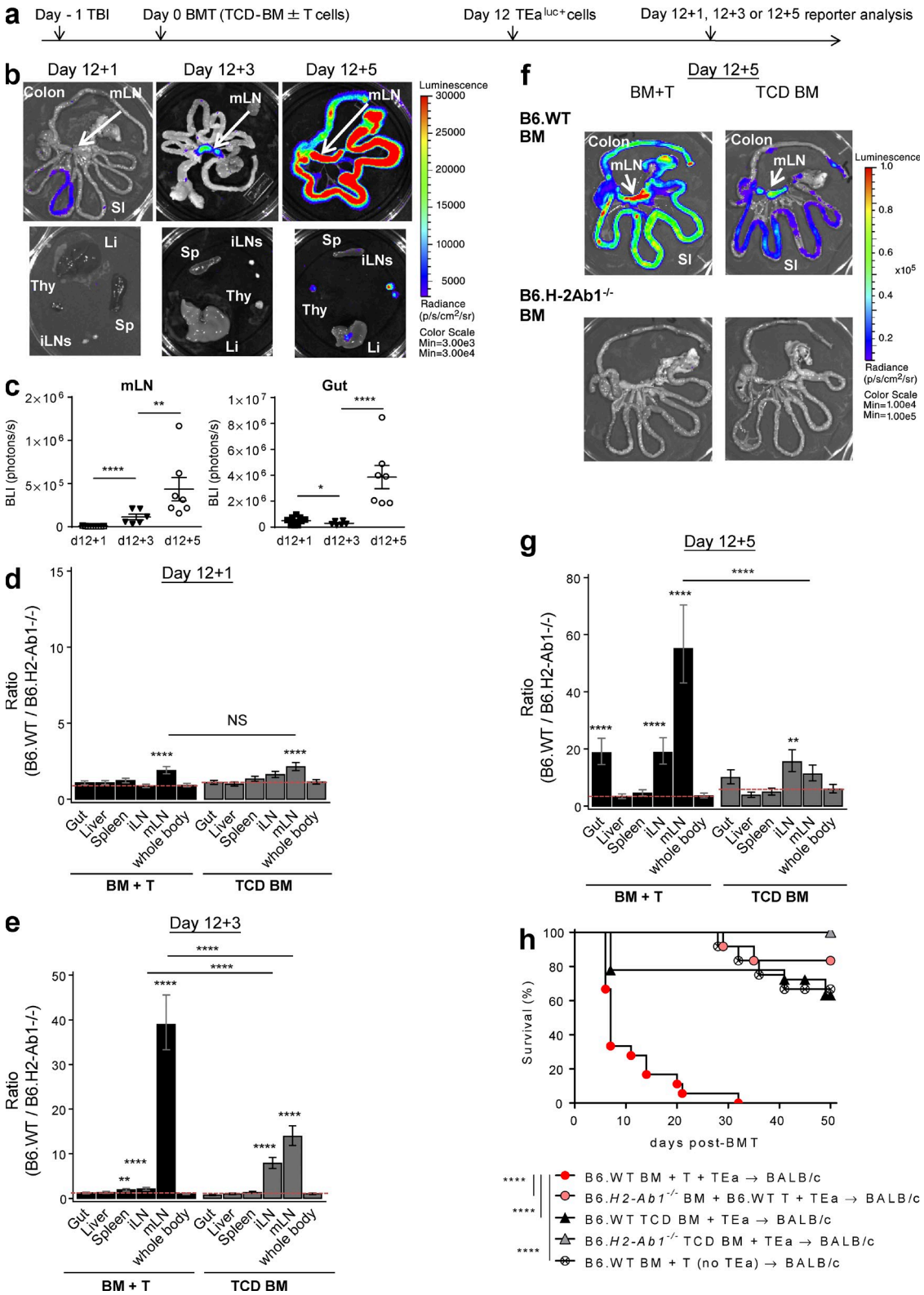

Figure 1. Donor alloantigen presentation during GVHD drives T cell accumulation and expansion in the mLNs. BALB/c mice were transplanted with TCD BM from B6.WT or B6.H2-Ab1$^{-/-}$ mice, with or without B6.WT T cells ("BM + T" or "TCD BM"). On day 12 TEa^{luc+} cells were injected, and 1, 3, or 5 d later BLI signals were quantified. (a) Experimental schema. (b and c) Representative images (b) and quantification (c) of BLI signals in mLNs and gut from the recipients of BM + T. Data shown are combined from three replicate experiments (n = 9, 6, and 7 per time point). ****, P < 0.0001; **, P = 0.0032; *, P = 0.035. Li, liver; SI, small intestine; Sp, spleen; Thy, thymus. (d–g) Ratio of BLI signals from the recipients of B6.WT BM to those from the recipients of B6.H2-Ab1$^{-/-}$ BM 1 (d), 3 (e), and 5 d

Published July 13, 2015

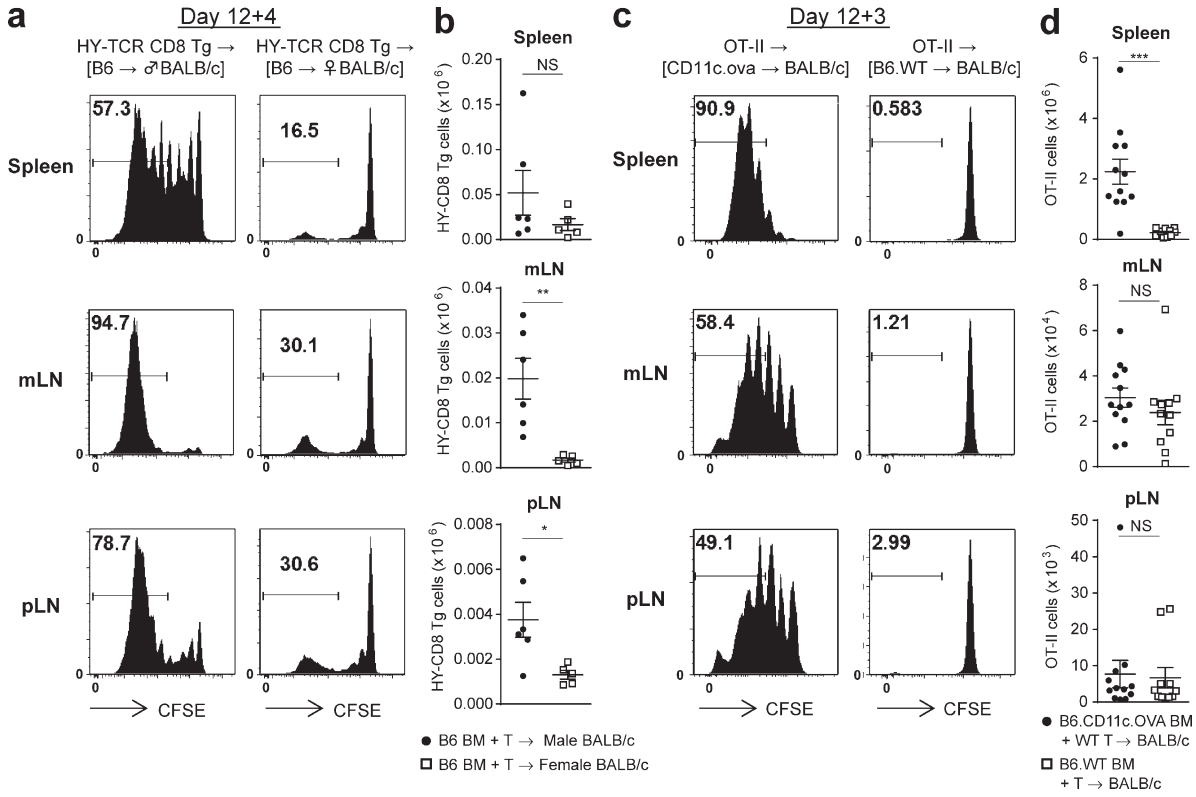

Figure 2. MHC class I–dependent alloantigen and third party antigen presentation in the mLNs. (a and b) Lethally irradiated female or male BALB/c recipients ($CD45.1^+CD45.2^-$) were transplanted with BM and T cells from female B6 ($CD45.1^+CD45.2^-$) mice. On day 12 female CFSE-labeled HY-TCR CD8 Tg cells ($CD45.1^-CD45.2^+$) were injected, and 4 d later spleen, mLNs, and iLNs were isolated. Representative CFSE dilution plots (a) and absolute numbers of HY-TCR CD8 Tg cells detected as $V\beta8^+CD8^+CD45.2^+$ cells (b). Data shown (n = 5–6 per group) are representative of two replicate experiments. **, P = 0.0043; *, P = 0.0209. (c and d) Lethally irradiated BALB/c recipients were transplanted with BM from B6.WT or B6.CD11c.ova mice and B6.WT T cells. On day 12 CFSE-labeled OT-II cells were injected, and 3 d later spleen, mLNs, and iLNs were isolated. Representative CFSE dilution plots (c) and absolute numbers of OT-II cells detected as $V\beta5^+V\alpha2^+CD4^+$ cells (d). Data shown are combined from two replicate experiments (n = 11–12 per group). ***, P = 0.0003. Data are represented as mean ± SEM.

responses, approaches targeting the whole donor APC compartment are likely to be deleterious, and a clear understanding of this process in total is needed to optimize appropriate therapeutic interventions. Here we delineate the temporal and spatial context of donor alloantigen presentation and uncover an unappreciated and critical role for acute GVHD in driving antigen presentation specifically within the GI tract that leads to a feed-forward cascade culminating in lethality.

RESULTS

Donor alloantigen presentation during GVHD drives T cell expansion in the mesenteric LNs (mLNs)

We developed a model of GVHD whereby the donor T cell response is directed to a single host allogeneic peptide presented within donor MHC class II. This system utilizes a B6-derived TEa TCR transgenic $CD4^+$ T cell that expresses luciferase and possesses a TCR specific for (BALB/c) host-derived $I\text{-}E^d$ peptide when presented within the (B6) donor $I\text{-}A^b$ molecule (Ochando et al., 2006; Markey et al., 2009; Koyama et al., 2012). To delineate the mechanisms by which donor APCs maintain acute GVHD, WT B6 or $I\text{-}A^b$–deficient B6 (B6.$H2Ab1^{-/-}$) donor BM was transplanted, with or without B6.WT T cells, into lethally irradiated BALB/c recipients. The B6.WT T cells initiate GVHD in response to host APCs in this system regardless of the expression of MHC class II within donor APCs (Koyama et al., 2012). 12 d later, when donor-derived APCs had reconstituted, luciferase-expressing TEa (TEa^{luc+}) cells were transferred. In this model, the TEa cells can respond only to host alloantigen presented within donor MHC class II ($I\text{-}A^b$). TEa expansion is thus a measurement of

(g) after TEa^{luc+} cell injection by mixed-model analysis and representative images on day 12 + 5 (f). ****, P < 0.0001; **, P = 0.001 (day 12 + 3, BM + T); **, P = 0.004 (day 12 + 5, TCD BM) versus whole body (d, e, and g), except BM + T versus TCD BM for mLNs or iLNs, P = 0.51 (d) and ****, P < 0.0001 (g and e). Data shown are combined from two replicate experiments, respectively (n = 10 [d], 7–12 [e], and 7–11 [g] per group). (h) BALB/c mice were transplanted with TCD BM from B6.WT or B6.H2-$Ab1^{-/-}$ mice with or without B6.WT T cells and/or TEa^{luc+} cells on day 0. GVHD survival is combined from three replicate experiments (n = 18 per group in groups of B6.WT BM with TEa and 12 in the other groups). ****, P < 0.0001 as indicated. Data are represented as mean ± SEM.

Published July 13, 2015

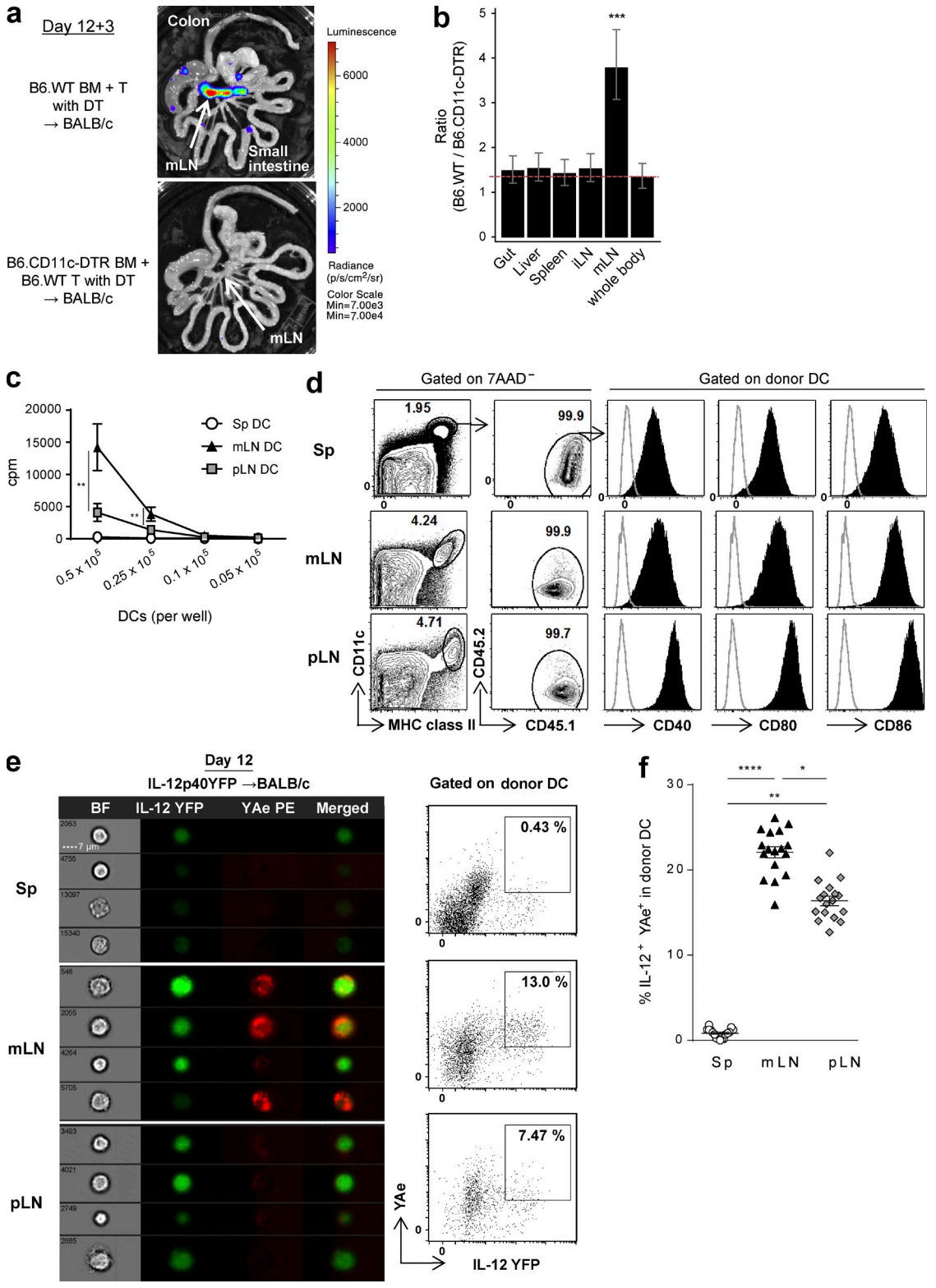

Figure 3. Alloantigen is preferentially presented by donor DCs in the mLNs during GVHD. (a and b) BALB/c mice were transplanted with TCD BM from B6.WT or B6.CD11c.DTR mice and B6.WT T cells, followed by DT administration. TEa^{luc+} cells injected on day 12 were quantified 3 d later. (a) Representative images. (b) The ratio of BLI signals from donor DC-replete mice to those from DC-deleted mice by mixed-model analysis are combined from two replicate experiments (n = 9 per group). ***, P = 0.00016 versus whole body. (c) Proliferation of TEa cells stimulated with DCs isolated at day 12 from BALB/c recipient mice transplanted with BM and T cells from B6.WT mice, as determined by [^{3}H]thymidine uptake. **, P = 0.0020 (DC; 5 × 10^4) or 0.0065 (DC; 2.5 × 10^4); mLN

Published July 13, 2015

indirect alloantigen presentation by donor APCs in isolation and is quantified by bioluminescence imaging (BLI; Fig. 1 a). We first analyzed the temporal and spatial presentation of alloantigen by donor APCs in recipients with or without acute GVHD. Although TEa cells were seen in the GI tract 1 d after injection, they exclusively accumulated within the mLNs within 3 d of injection and subsequently expanded therein. Within 5 d of injection, they had redistributed into the GI tract (Fig. 1, b and c).

To compare the relative importance of indirect alloantigen presentation within individual organs, we calculated the average ratio of each organ to its "control," that is, the recipients of B6.H2Ab1$^{-/-}$ BM grafts where alloantigen presentation by donor APCs was absent and the BLI signal from TEa cells reflected homeostatic proliferation. We then used mixed-model analysis (Cochran and Cox, 1957) to allow us to compare organs from the same mouse. This demonstrated that 1 d after injection TEa cells distribute almost equally between organs, with only the mLNs demonstrating an alloantigen-specific signal, an effect independent of GVHD at this time point (Fig. 1 d). 3 d after injection, this alloantigen-specific signal in the mLNs had further amplified in animals with GVHD, with moderate signals now detectable in mLNs and inguinal LNs (iLNs) in animals without GVHD (Fig. 1 e). By day 5, an alloantigen-specific signal was also seen in the GI tract (Fig. 1, f and g) in the animals with GVHD, and thus GVHD itself resulted in enhanced indirect alloantigen presentation in the mLNs and GI tract (Fig. 1, e and g). To confirm that GVHD could itself induce indirect alloantigen presentation and aggravate GVHD once initiated by host APCs, TEa cells were transplanted into BALB/c recipients with or without B6.WT T cells on day 0. Surprisingly, the initiation of GVHD by host APCs induced lethal disease thereafter that was driven primarily by donor antigen presentation (Fig. 1 h). These data suggest that, in the presence of GVHD, the mLN is a preferential site of indirect alloantigen presentation early after BM transplant (BMT), and this precedes the infiltration of alloreactive donor T cells into the GI tract.

We next examined whether this phenomenon held true for CD8$^+$ T cells responding to recipient alloantigen presented within donor MHC class I. Male or female BALB/c.CD45.1$^+$ recipients were transplanted with BM and T cells from B6.CD45.1$^+$ mice and 12 d later injected with CFSE-labeled B6.CD45.2$^+$ H-2D^b–restricted HY-reactive transgenic CD8$^+$ reporter T cells (HY-TCR CD8 Tg) that react exclusively to recipient male antigen presented with donor MHC class I (H-2D^b). HY-TCR CD8 Tg cells accumulated again in the mLNs of male BMT recipients 4 d after transfer (Fig. 2, a and b). In contrast, only homeostatic proliferation was seen in female recipients. To compare these findings with alloantigen to a third party antigen, BALB/c mice were transplanted with BM from B6.WT or B6.CD11c-OVA transgenic mice (where OVA is driven by the CD11c promoter and is not derived from host) and B6.WT T cells. In this setting, the highest levels of OVA-specific OT-II proliferation and expansion were observed in spleen (Fig. 2, c and d), with only low-level homeostatic proliferation in the recipients of WT BM. These data confirm alloantigen to be preferentially presented by donor APCs within the mLNs, particularly within MHC class II.

Alloantigen is preferentially presented by donor DCs in the mLNs during GVHD

We next analyzed the role of donor DCs in the organ-specific indirect alloantigen presentation because they have been suggested as the primary APCs responsible for indirect alloantigen presentation (Markey et al., 2009). Lethally irradiated BALB/c mice were transplanted with BM from B6.WT or B6.CD11c-DTR mice (where diphtheria toxin [DT] receptor [DTR] is driven by CD11c promoter) and B6.WT T cells, and DT was administered to deplete donor DCs. The absence of donor DCs elicited a striking reduction in T cell expansion, again primarily within the mLNs (Fig. 3, a and b), suggesting that donor DCs were indeed the crucial APCs presenting alloantigen at this site. To further confirm this specialized ability of donor DCs within the mLNs to induce alloreactive T cell responses, donor DCs from mLNs, peripheral LNs (pLNs), and spleen of transplanted BALB/c recipients were purified after BMT and co-cultured with TEa cells ex vivo. This confirmed that the highest level of alloantigen presentation in donor DCs was from mLNs (Fig. 3 c). This did not appear related to differences in activation because costimulatory molecule expression (CD40, CD80, or CD86) was not specifically increased in DCs in the mLNs (Fig. 3 d). Because acute GVHD in the GI tract is a Th1 (and to a lesser extent Th17)-driven disease (Markey et al., 2014), we investigated whether cytokines such as IL-12, secreted by DCs, may be providing costimulatory signals in the mLNs. Imaging and conventional flow cytometric analysis indeed confirmed high levels of IL-12p40 and alloantigen presentation (YAe$^+$) by donor DCs specifically within the mLNs (Fig. 3, e and f).

The mLN CD103$^+$CD11b$^-$ DC subset presents alloantigen and secretes IL-12

We next determined which DC subsets were critical for indirect alloantigen presentation. Subset analysis of donor DCs in

versus pLN. ****, P < 0.0001 (DC; 5 × 10^4, 2.5 × 10^4); mLN versus spleen (Sp). (d) Representative FACS plots at day 12 after BMT of BALB/c (CD45.2$^+$) recipients receiving BM and T cells from B6.CD45.1$^+$ mice. (c and d) Data are representative of two replicate experiments. (e and f) BALB/c mice (I-A^{d+}) were transplanted with BM and T cells from B6.IL-12p40YFP mice. Donor DCs (IA/IE$^+$CD11c$^+$I-A^{d-}7AAD$^-$) from spleen, mLNs, and pLNs were FACS sorted (e) or unsorted (f) on day 12. (e) Representative pictures (left) and quantification (right) of imaging flow cytometry for IL-12p40YFP and YAe are shown from three replicate experiments. (f) The frequency of YFP$^+$YAe$^+$ cells in the IA/IE$^+$CD11c$^+$I-A^{d-}7AAD$^-$ population was quantified by conventional flow cytometry. Data shown are combined from three replicate experiments (n = 17). ****, P < 0.0001; **, P = 0.0011; *, P = 0.0118. Data are represented as mean ± SEM.

Published July 13, 2015

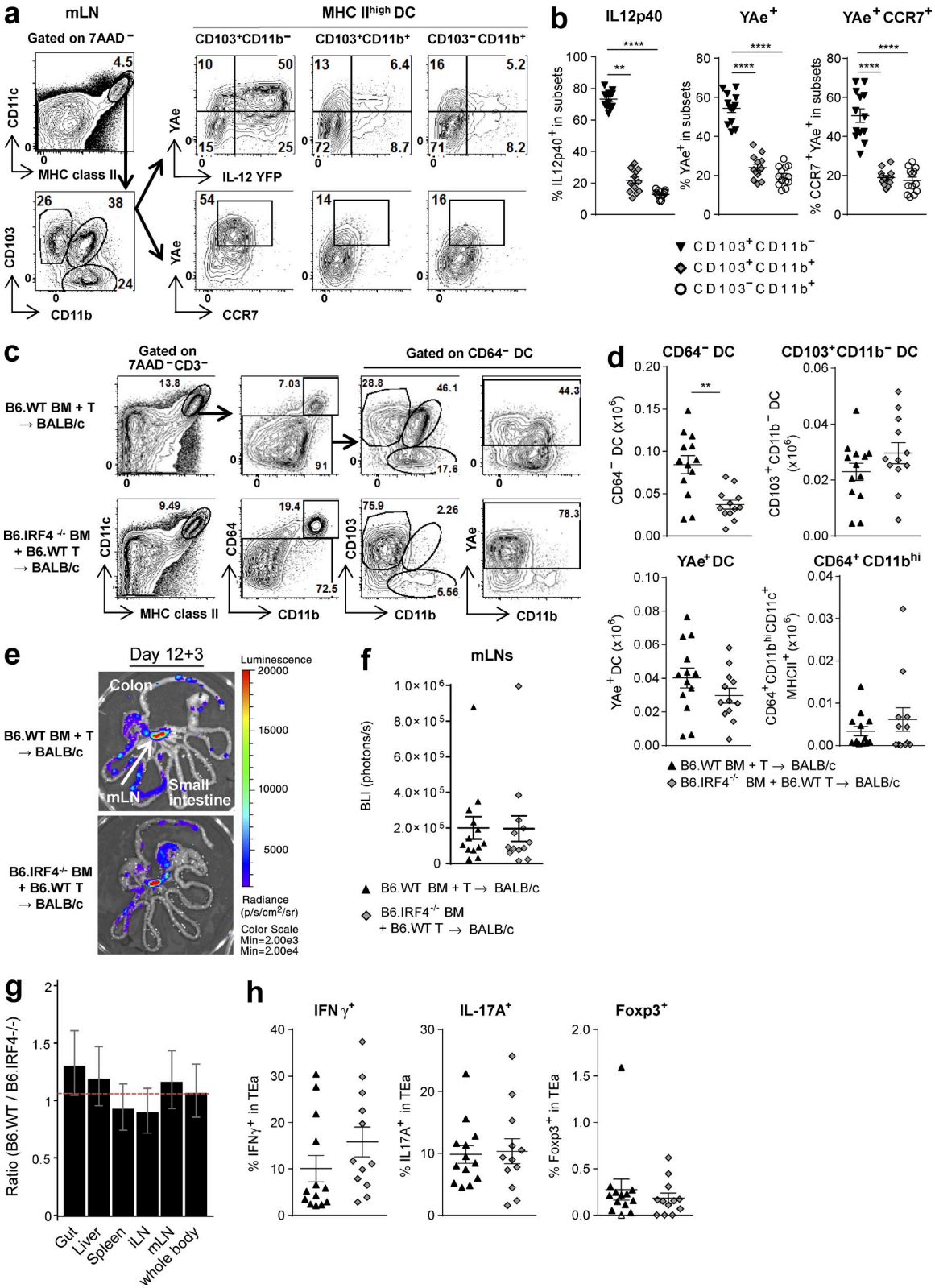

Figure 4. The mLN CD103⁺CD11b⁻ DC subset presents alloantigen and secretes IL-12. (a and b) BALB/c mice were transplanted with BM and T cells from B6.IL-12p40-YFP mice. mLNs were isolated on day 12. Representative FACS plots (a) and quantification (b) of YFP, YAe, or CCR7 expression on DC subsets discriminated by CD103 and CD11b expression. Data shown are combined from two replicate experiments (n = 13). ****, $P < 0.0001$; **, $P = 0.0031$. (c–h) BALB/c mice were transplanted with TCD BM from B6.WT or B6.IRF4$^{-/-}$ mice and B6.WT T cells. On day 12 TEa^{luc+} cells were injected, and 3 d

Published July 13, 2015

the mLNs discriminated three subsets as $CD103^+CD11b^-$, $CD103^+CD11b^+$, and $CD103^-CD11b^+$ and demonstrated that the $CD103^+CD11b^-$ DCs included the highest frequency of alloantigen-presenting and IL12p40-producing cells that concurrently express high levels of CCR7 (Fig. 4, a and b). This led us to hypothesize that donor $CD103^+CD11b^-$ DCs may migrate from the GI tract of animals with GVHD to the mLNs and prime alloreactive T cells.

To examine whether antigen presentation in the mLNs was dependent on the $CD103^+CD11b^-$ DC subset, we used B6.IRF4$^{-/-}$ mice as BMT donors because they lack the $CD103^+CD11b^+$ DC subset in the mLNs and the lamina propria (Persson et al., 2013; Schlitzer et al., 2013). Donor DCs reconstituted from B6.IRF4$^{-/-}$ BM were predominantly of the $CD103^+CD11b^-$ DC subset (Fig. 4 c). Marked reductions in both $CD11b^+$ subsets were seen, resulting in an overall reduction in DC numbers (Fig. 4 d). However, the total numbers of $CD103^+CD11b^-$ DCs and alloantigen-presenting (YAe^+) DCs were comparable with those in recipients of B6.WT BM (Fig. 4 d). Of note, $CD64^+CD11b^{hi}$ macrophages were also comparable between groups. This strategy thus allowed us to study the function of the donor $CD103^+CD11b^-$ DC subset after BMT, largely in isolation. As predicted, indirect alloantigen presentation in the mLNs and all other analyzed organs was equivalent in recipients of B6.IRF4$^{-/-}$ and B6.WT BM (Fig. 4, e–g), despite the lack of $CD11b^+$ DCs. Furthermore, the $CD103^+CD11b^-$ DC subset was sufficient to drive T cell differentiation within the mLNs (Fig. 4 h).

$CD64^+CD11b^{hi}$ macrophages are dispensable for alloantigen presentation

Given that $CD64^+CD11b^{hi}CD11c^+$MHC class II^+ macrophages have been reported as important APCs in T cell–dependent colitis models (Tamoutounour et al., 2012), we determined whether this subset was also involved in indirect alloantigen presentation after BMT. Analysis of donor $CD11c^+$MHC class II^+ cells in the mLNs demonstrated that $CD64^+CD11b^{hi}$ macrophages express high levels of the C-C chemokine receptor 2 (CCR2) and CD115 (the CSF-1 receptor [CSF-1R]). In contrast, and as expected, expression of CCR2 and CD115 by the $CD64^-$ DC subsets was negligible (Fig. 5 a; Tamoutounour et al., 2012; Alexander et al., 2014). Consistent with this, $CD64^+CD11b^{hi}$ macrophage reconstitution in the mLNs of BMT recipients of B6.CCR2$^{-/-}$ BM was profoundly impaired, whereas reconstitution of all DC subsets was intact (Fig. 5, b and c). In spite of this inhibition in macrophage reconstitution, indirect alloantigen-specific T cell expansion in the mLNs was comparable in recipients of CCR2$^{-/-}$ BM and enhanced within the gut (Fig. 5, d–f). We confirmed this result using B6.WT BM or B6.CSF-1R$^{-/-}$ BM, which was isolated from fetal liver chimeras (FLCs) because CSF-1R deficiency is neonatally lethal in B6 mice. $CD64^+CD11b^{hi}$ macrophages were again specifically reduced in the recipients of B6.CSF-1R$^{-/-}$ BM and alloantigen-specific T cell expansion was again intact in the mLNs and increased in the gut, relative to recipients of B6.WT FLC BM (Fig. 5, g–i). Thus, donor $CD64^+CD11b^{hi}$ macrophages are not required for indirect alloantigen presentation and, consistent with previous studies (MacDonald et al., 2010; Hashimoto et al., 2011), are likely to play a suppressive role in acute GVHD.

Damage-associated molecular pattern (DAMP)/pathogen-associated molecular pattern (PAMP) signals drive alloantigen presentation by donor $CD103^+CD11b^-$ DCs

We next investigated the factors responsible for the high levels of indirect alloantigen presentation by donor DCs within the mLNs. The mLN drains the GI tract, which contains large numbers of PAMPs and DAMPs from tissues damaged by GVHD, which are sensed by pattern recognition receptors (PRRs). These pathways can stimulate antigen presentation (Saleh and Trinchieri, 2011; Kondo et al., 2012). TLR signaling through myeloid differentiation protein-88 (MyD88) or Toll–IL-1 receptor domain–containing adaptor inducing IFN-β (TRIF) and receptor for advanced glycation end products (RAGE) are well-characterized PRRs (Yamamoto et al., 2003; Chen et al., 2008). We analyzed the contribution of DAMP/PAMP signaling to indirect alloantigen presentation by transplanting BALB/c recipients with BM from B6.MyD88$^{-/-}$TRIF$^{-/-}$ or B6.RAGE$^{-/-}$ donors. In the absence of these pathways, TEa expansion driven by indirect alloantigen presentation was decreased specifically within the mLN (Fig. 6, a–d). We also noted a significant reduction in the $CD103^+CD11b^-$ DC subset in the recipients of MyD88$^{-/-}$TRIF$^{-/-}$ or RAGE$^{-/-}$ BM and an associated reduction in YAe^+ and IL-12p40–secreting DCs in the mLN (Fig. 6, e–g). The number of $CD64^+CD11b^{hi}$ macrophages was not influenced by the absence of MyD88/TRIF or RAGE signaling. These data confirm that donor $CD103^+CD11b^-$ DCs in the mLNs present alloantigen and secrete IL-12p40 in response to DAMP/PAMP signals.

Donor-derived IL-12 and IL-6 drive T cell expansion and differentiation in the mLNs in an alloantigen presentation–independent manner

Although DAMPs/PAMPs increase cytokine production and alloantigen presentation of donor DCs, particularly

later DC subsets and TEa expansion were analyzed. (c and d) Representative FACS plots (c) and absolute numbers of $CD64^-$ DCs, $CD103^+CD11b^-$ DCs, YAe^+CD64^- DCs, and $CD64^+CD11b^{hi}CD11c^+$MHC class II^+ cells in mLNs (d) are shown. **, P = 0.0011; P = 0.1979 ($CD103^+CD11b^-$ DC), P = 0.1900 (YAe^+ DC), P = 0.28 ($CD64^+CD11b^{hi}$). (e and f) Representative images (e) and quantification (f) of BLI signals. P = 0.8310. (g) Ratio of BLI signals from B6.WT BM recipients to those from B6.IRF4$^{-/-}$ BM recipients by mixed-model analysis. (h) Frequency of IFN-γ, IL-17A, and Foxp3 expression gated on TEa cells detected as $V\beta6^+V\alpha2^+CD45.1^+$ cells. P = 0.1283 (IFN-γ), P = 0.8343 (IL-17A), P = 0.4597 (Foxp3). (c–h) Data shown are combined from two replicate experiments (n = 13 per group). Data are represented as mean ± SEM.

Published July 13, 2015

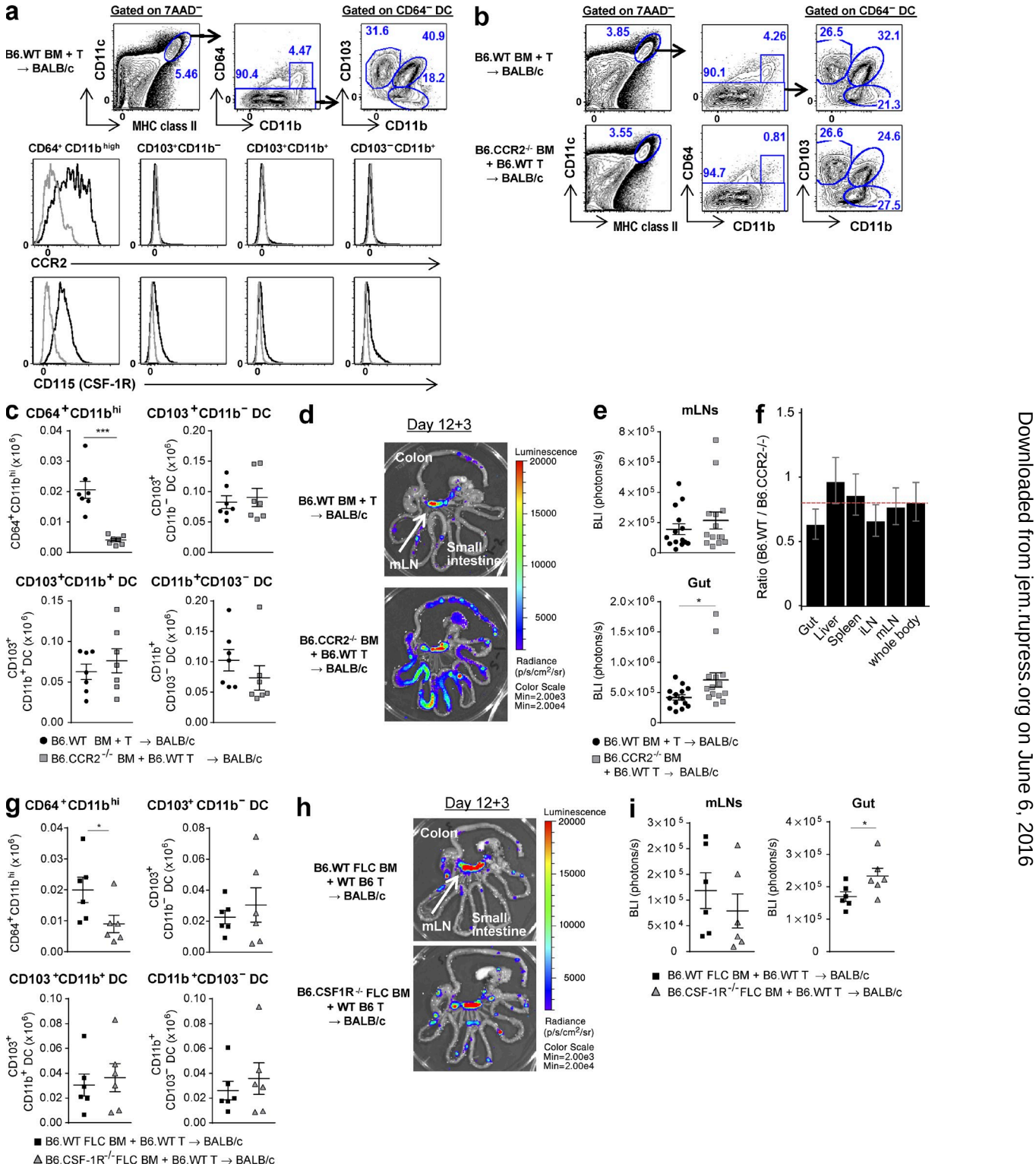

Figure 5. mLN CD64⁺CD11b^hi macrophages are not required for indirect alloantigen presentation. (a–f) BALB/c mice were transplanted with TCD BM from B6.WT or B6.CCR2$^{-/-}$ mice and B6.WT T cells. On day 12 TEa^{luc+} cells were injected, and 3 d later DC subsets and TEa expansion were analyzed. (a) Representative FACS plots for the gating strategy (top), CCR2 expression (middle), and CD115 expression (bottom) on CD64⁺CD11b^{hi}, CD103⁺CD11b⁻, CD103⁺CD11b⁺, and CD103⁻CD11b⁺ subsets in the mLNs from recipients of B6.WT BM. Gray histograms show isotype control. (b and c) Representative FACS plots (b) and absolute numbers (c) of the aforementioned subsets from the mLNs. ***, P = 0.0006 (CD64⁺CD11b^{hi}); n = 7 per group. (d and e) Representative images (d) and quantification (e) of BLI signals. P = 0.25 (mLN); *, P = 0.0138 (gut). (f) Ratio of BLI signals from B6.WT BM recipients to those from B6.

Published July 13, 2015

$CD103^+CD11b^-$ DCs, we sought to clarify whether concurrent cytokine release also influences donor T cell expansion and differentiation within the mLNs. The transplantation of B6.IL-12p40$^{-/-}$ BM confirmed that IL-12 indeed drove donor T cell expansion specifically in the mLNs (Fig. 7 a) and IL-12 promoted IFN-γ but not IL-17 nor Foxp3-expressing TEa cells (Fig. 7, b and c). Intriguingly, the effect on IFN-γ was independent of any quantitative change to alloantigen presentation by DCs in the mLNs (Fig. 7, d and e). Thus, IL-12 secretion by donor $CD103^+CD11b^-$ DCs in the mLNs directly promotes T cell expansion and differentiation. Next we tested the effect of IL-6 secretion from donor BM cells on donor alloantigen presentation because blocking of IL-6 receptor has shown promise in reducing the incidence and severity of acute GVHD, including that within the GI tract, in both preclinical studies (Chen et al., 2009; Tawara et al., 2011) and clinical trials (Kennedy et al., 2014). Among donor DCs, the $CD103^+CD11b^+$ subset expressed the highest levels of IL-6 mRNA (Fig. 7 f), consistent with studies in other disease settings (Persson et al., 2013; Schlitzer et al., 2013). However, IL-6 is also known to be produced by most other hematopoietic cells, especially after BMT, including prevalent myeloid (e.g., monocytes and neutrophils) and lymphoid lineages (Hirano, 1998; Varelias et al., 2015). Of note, Th17 cell differentiation was only observed in the mLNs, and we thus examined the effects of IL-6 on T cell responses at this site. Like IL-12, donor-derived IL-6 also increased TEa expansion in the mLNs, and this was an organ-specific effect (Fig. 7 g). IL-6 was required for Th17 cell differentiation, but this effect was again independent of any quantitative changes to alloantigen presentation by DCs in the mLNs (Fig. 7, h–k). Although the absence of indirect alloantigen presentation itself abrogated TEa expansion and differentiation in total (Figs. 1 and 8 a), the relative requirements of MHC class II for Th1 versus Th17 cell differentiation (cytokine-producing capacity) of TEa cells was different. IL-17 production was absolutely dependent on antigen presentation, whereas some IFN-γ production could still occur in the setting of homeostatic T proliferation within the mLNs, resulting in small numbers of Th1 cells (Fig. 8, a and b). Of note, this low-level homeostatic Th1 cell differentiation is insufficient to induce acute GVHD (Fig. 1 h; Koyama et al., 2012). Thus, alloantigen presentation is crucial for full T cell expansion and differentiation during GVHD.

These results demonstrate that DAMP/PAMP signals generated during GVHD enhance alloantigen presentation and cytokine production by donor DCs within the mLNs, which promote alloreactive T cell expansion and differentiation therein, before donor T cell migration into the GI tract.

Donor DCs presenting alloantigen expand in the colon during GVHD

To evaluate donor DC reconstitution in the presence or absence of GVHD in a quantitative fashion, BALB/c mice were transplanted with BM from B6.CD11c.GCDL mice (luciferase expression is driven off the CD11c promoter) with or without B6.WT T cells. BLI was then used to quantify donor $CD11c^+$ DC reconstitution thereafter (Fig. 9 a). The presence of GVHD increased donor DC expansion in the second week after BMT within both the mLNs and the GI tract (Fig. 9, b and c). However, this expansion of donor DCs in animals with GVHD was not organ specific at day 12 after BMT (Fig. 9 d) and so did not account for the tropism of indirect alloantigen presentation for the mLNs. Interestingly, the increase in donor DC expansion in recipients with GVHD was seen in the colon but not the small intestine beyond day 12 (Fig. 9 c). We thus speculated that donor DCs within the colon may differ functionally in their capacity to present alloantigen to those in the small intestine. Indeed, only colonic DCs were presenting alloantigen (YAe^+) and expressing IL-12p40 (Fig. 9 e). Furthermore, these DCs only occurred in the colon in the presence of GVHD. Indirect alloantigen presentation was seen within the $CD103^+CD11b^-$ subset (30% of this fraction), the $CD103^-CD11b^+$ subset, and $CD64^+CD11c^+$ macrophages (15% of each fraction). IL-12p40 production was largely restricted to the $CD103^+CD11b^-$ subset (Fig. 9 e). These data support the notion that the $CD103^+CD11b^-$ DC subset in the colon may play the major role in alloreactive T cell activation and expansion, either locally or within the mLNs after migration. In contrast, indirect alloantigen presentation by donor DCs in the small intestine is minimal.

Colon-derived donor DCs migrate to the mLNs via CCR7 and imprint the α4β7 gut-homing integrin on donor T cells

Because donor T cells rapidly gain access to the GI tract after BMT, we next sought to establish whether the initial site of antigen presentation by donor APCs to donor T cells was in the mLNs or the colon itself. Donor DCs within the mLNs express high levels of CCR7 (Fig. 4 a), and we thus used CCR7$^{-/-}$ donors in BMT experiments to understand the migratory properties and origin of DCs at this site. Interestingly, the absence of CCR7 specifically ablated nearly all donor DC subsets (MHC class $II^+CD11c^+CD64^-$) within the mLNs after BMT with a resultant accumulation of YAe^+ DCs in the colon (Fig. 10, a and b). The number of $CD64^+CD11b^{hi}$ macrophages was not influenced by the absence of CCR7. The absence of CCR7 ablated indirect alloantigen presentation and T cell priming specifically in the mLNs (Fig. 10, c–e)

CCR2$^{-/-}$ BM recipients by mixed-model analysis. Data shown are combined from two replicate experiments (n = 14 per group). (g–i) BALB/c mice were transplanted with TCD BM from B6.WT FLC mice or B6.CSF1R$^{-/-}$ FLC mice with B6.WT T cells. On day 12 TEa^{luc+} cells were injected, and 3 d later DC subsets and TEa expansion were analyzed. (g) Absolute numbers of the aforementioned subsets from the mLNs are shown. *, P = 0.0152 ($CD64^+CD11b^{hi}$). (h and i) Representative images (h) and quantification (i) of BLI signals. P = 0.30 (mLN); *, P = 0.04 (gut). (g–i) n = 6 per group. Data are represented as mean ± SEM.

Published July 13, 2015

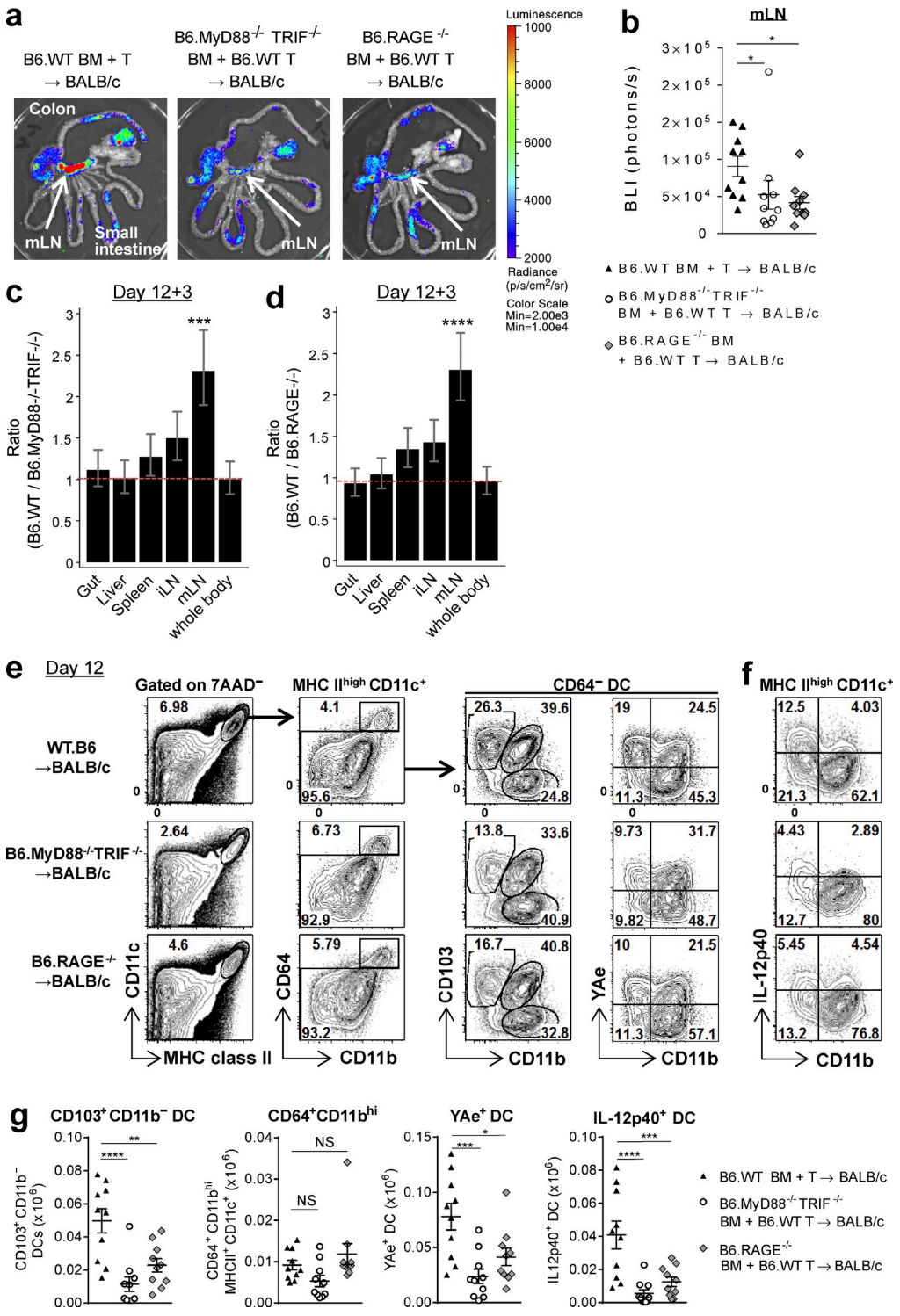

Figure 6. DAMP/PAMP signals drive alloantigen presentation by the donor CD103⁺CD11b⁻ DC subset within the mLNs. BALB/c mice were transplanted with TCD BM from B6.WT, B6.MyD88$^{-/-}$TRIF$^{-/-}$, or B6.RAGE$^{-/-}$ mice with B6.WT T cells. (a–d) On day 12 TEa^{luc+} T cells were injected, and 3 d later BLI signals were measured. Representative image (a), quantification of BLI signals in mLNs (b), and ratio of BLI signals from B6.WT BM recipients to those from B6.MyD88$^{-/-}$TRIF$^{-/-}$ (c) or B6.RAGE$^{-/-}$ (d) BM recipients by mixed-model analysis. Data shown are combined from two replicate experiments (n = 10 per group). *, P = 0.0186, B6.WT BM versus B6.MyD88$^{-/-}$TRIF$^{-/-}$ BM; *, P = 0.0187, B6.WT BM versus B6.RAGE$^{-/-}$ BM (b). ***, P = 0.00027 (c); ****, P < 0.0001 (d), mLN versus whole body. (e–g) mLNs were isolated on day 12. Representative FACS plots (e and f) and absolute numbers of CD103⁺CD11b⁻ DC, YAe⁺ DC, IL-12p40⁺ DC, and CD64⁺CD11b^{hi} macrophages in the mLNs (g). Data shown are combined from two replicate experiments (n = 10 per group). ****, P < 0.0001; **, P = 0.0025; *, P = 0.0131. ***, P = 0.0004, B6.WT BM versus B6.MyD88$^{-/-}$TRIF$^{-/-}$ BM (YAe⁺ DC); ***, P = 0.0001, B6.WT BM versus B6.RAGE$^{-/-}$ BM (IL-12p40⁺DC (g). Data are represented as mean ± SEM.

Published July 13, 2015

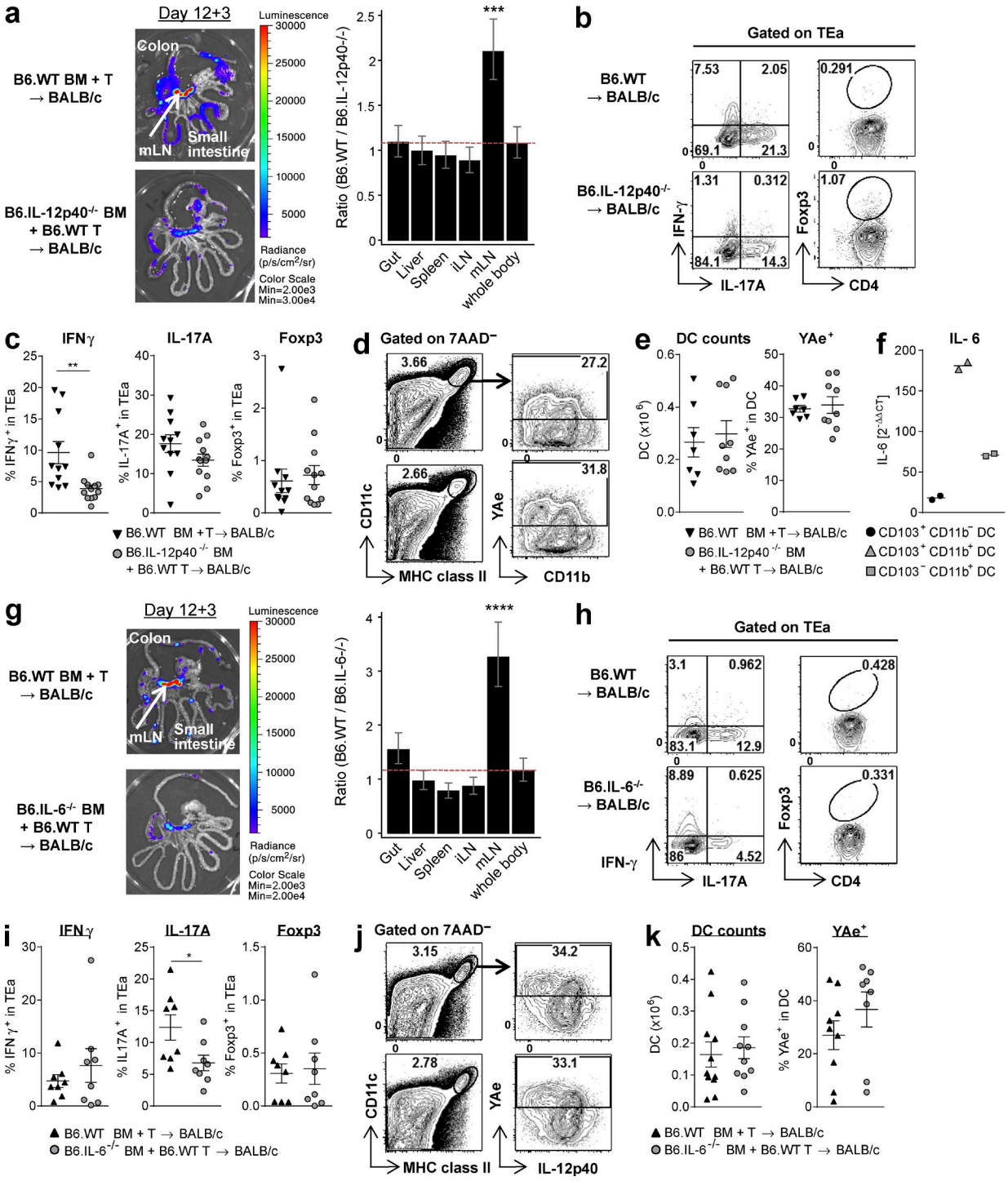

Figure 7. Donor-derived IL-12 and IL-6 drive T cell expansion and differentiation in the mLNs. BALB/c mice were transplanted with TCD BM from B6.WT or B6.IL-12p40$^{-/-}$ mice (a–e) or B6.IL-6$^{-/-}$ mice (g–k) with B6.WT T cells. TEa^{luc+} cells were injected on day 12, and readouts were measured 3 d later in mLNs. (a and g) Representative BLI pictures (left) and ratio of BLI signals from B6.WT BM recipients to those from B6.IL-12p40$^{-/-}$ BM recipients (a) or B6.IL-6$^{-/-}$ BM recipients (g) by mixed-model analysis (right). ***, P = 0.00071 (a); ****, P < 0.0001 (g) mLN versus whole body. Data shown are combined from two replicate experiments (n = 12 [a] or 11 [g] per group). (b, c, h, and i) Representative FACS plots (b and h) and quantification (c and i) of IFN-γ, IL-17A, and Foxp3 expression gated on TEa cells. **, P = 0.0020 for IFN-γ (c); *, P = 0.0396 for IL-17A (i). Data shown are combined from two replicate experiments (n = 11–12 [b and c] or 8 [h and i] per group). (d, e, j, and k) Representative FACS plots (d and j) and quantification (e and k) of absolute number of DCs and their YAe expression. Data shown are combined from two replicate experiments (n = 7–9 [d and e] or 10–11 [j and k] per group). Data are represented as mean ± SEM. (f) BALB/c mice were transplanted with TCD BM and T cells from B6.CD45.1+ mice, and DC subsets were isolated by FACS sorting of mLNs combined from five mice on day 12. IL-6 quantitative RT-PCR was performed. Data are shown from two separate experiments, each combining mLNs from five mice. Means are shown.

Published July 13, 2015

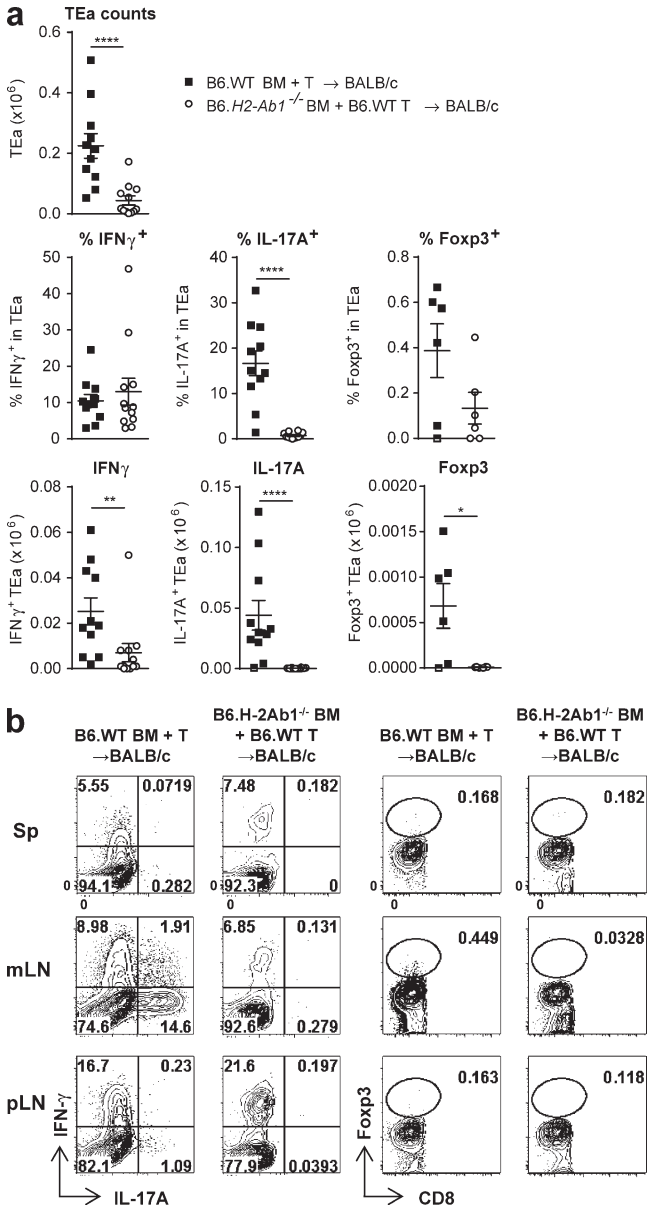

Figure 8. T cell expansion and differentiation are dependent on indirect antigen presentation. BALB/c mice were transplanted with TCD BM from B6.WT or B6.*H2-Ab1*$^{-/-}$ mice and B6.WT T cells. On day 12 TEa T cells were injected, and 3 d later TEa cells from spleen (Sp), mLNs, and pLNs were quantified. (a) Quantification of absolute number of TEa cells (Vb6$^+$Va2$^+$CD8$^-$CD90.2$^+$) and frequency and absolute numbers of IFN-γ–, IL-17A–, and Foxp3-expressing TEa cells in mLNs. (b) Representative FACS plots. Data shown are combined from two replicate experiments (n = 11–12 per group for TEa counts, IFN-γ, and IL-17A; n = 6 per group for Foxp3). ****, P < 0.0001; **, P = 0.0032; *, P = 0.041. Data are represented as mean ± SEM.

and prevented the migration of donor T cells into the GI tract and systemically thereafter (Fig. 10, f and g). We confirmed the requirement for CCR7 in DC migration into the mLNs in an MHC-matched, minor histocompatibility antigen (miHA)-mismatched BMT model of GVHD (B6→BALB/b; Fig. 10 h). Furthermore, DAMP/PAMP signaling also expanded the proportion of CD103$^+$CD11b$^-$ DCs in the mLNs in this system (Fig. 10 h). In the MHC disparate system, TEa cells in the mLNs from the recipients of CCR7$^{-/-}$ BM were markedly reduced versus recipients of WT BM (0.08 ± 0.03 vs.1.76 ± 0.36 × 10^5/mLN, P < 0.0001), with significantly reduced numbers of IFN-γ$^+$, IL-17A$^+$, and Foxp3$^+$ cells (not depicted), similar to that seen in recipients of MHC class II$^{-/-}$ BM (Fig. 8, a and b). Furthermore, TEa cells in the mLNs in recipients of CCR7$^{-/-}$ BM failed to express α4β7 integrin, which was also noted in recipients of MHC class II$^{-/-}$ BM (Fig. 10, i and j). Thus, donor alloantigen-presenting DCs migrate from the colon into the mLNs where they initiate T cell priming and differentiation and imprint an integrin expression pattern that drives migration into the intestine to induce lethal GVHD.

DISCUSSION

Here we delineate the organ-specific amplification of indirect alloantigen presentation by GVHD and the dynamics of the APC subsets involved therein. Surprisingly, GVHD initiated by recipient APCs markedly enhanced alloantigen presentation within the mLNs by donor CD103$^+$CD11b$^-$ DCs that drive lethal GVHD. Although the presence of GVHD can impair systemic antigen presentation by the donor CD11b$^+$ DC subset outside of the GI tract (Markey et al., 2012), the impact of GVHD on antigen presentation has not been investigated in an organ-specific manner previously. Here we show that GVHD increases and maintains donor DC reconstitution specifically in the colon and the mLNs. Furthermore, GVHD profoundly enhances the ability of colonic CD103$^+$CD11b$^-$ DCs to present alloantigen and secrete IL-12, before their CCR7-dependent migration into the mLNs. Within the mLNs these DCs expand, differentiate, and imprint an integrin signature on alloreactive T cells, which result in the accumulation of pathogenic Th1 cells in the GI tract, culminating in fulminant GVHD (depicted in Fig. S1). It is likely that donor T cells emigrating to the colon will encounter tissue DCs presenting alloantigen therein and undergo further activation, differentiation, and cytokine release in situ. Because donor T cells in this system cannot make cognate interaction with target tissue by virtue of their TCR-MHC restriction, the exacerbation of GVHD will instead be mediated by inflammatory cytokines, consistent with this as a known dominant pathway in CD4-dependent GVHD (Teshima et al., 2002).

DAMP/PAMP signaling via TLRs has been recognized to play a crucial role in GVHD (Blazar et al., 2012; Heidegger et al., 2014) caused by donor cells (Cooke et al., 1998), an effect thought to be via the induction of proinflammatory cytokines. Here we demonstrate that a major effect of these DAMPs/PAMPs through MyD88/TRIF signaling is to enhance alloantigen presentation. We also confirm a similarly important role for the RAGE pathway. Our data also demonstrate that the DAMP/PAMP signals influence not only the function but also the expansion of donor CD103$^+$CD11b$^-$ DCs. In contrast, recipient hematopoietic APCs are in a state

Published July 13, 2015

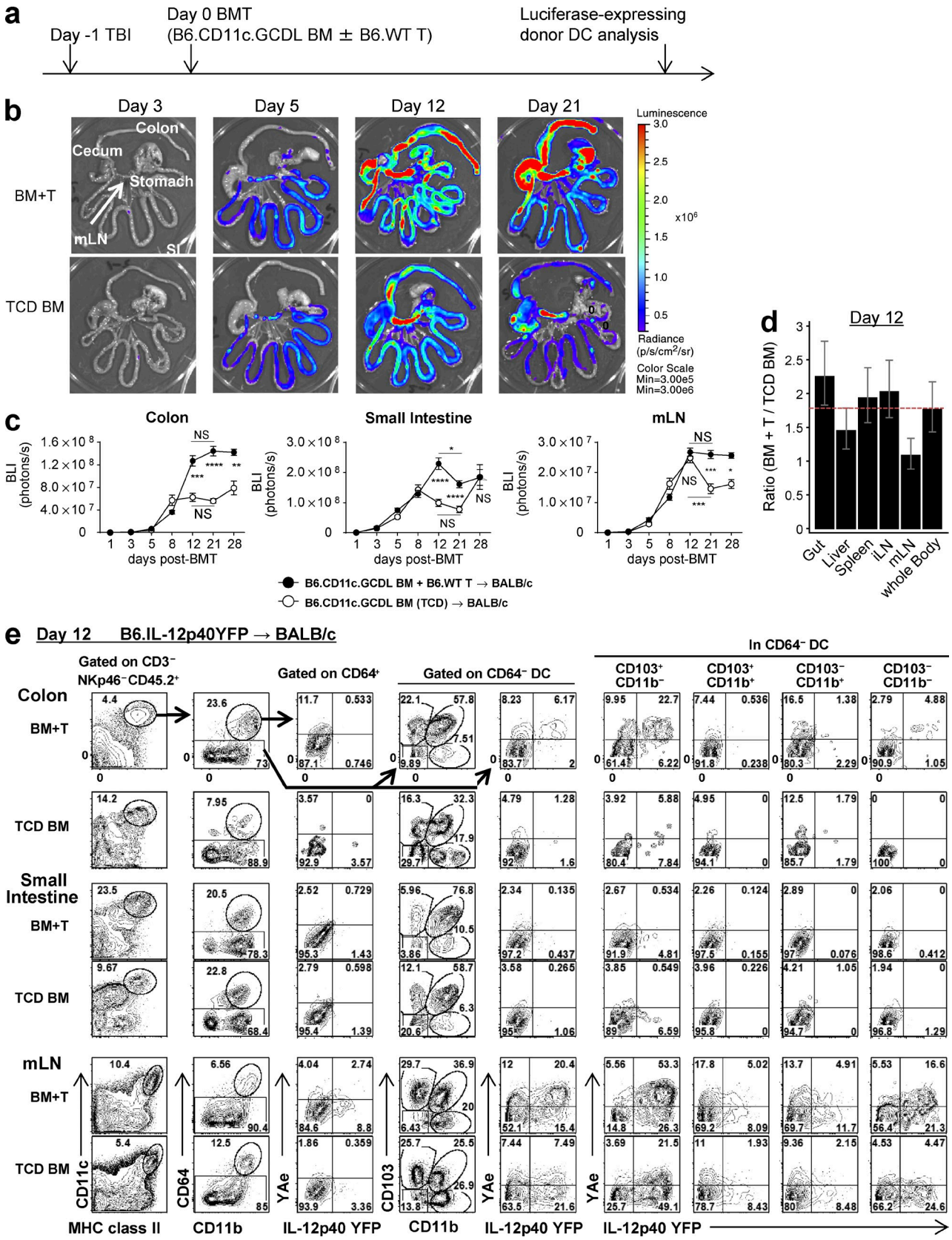

Figure 9. Donor DCs presenting alloantigen expand in the colon during GVHD. (a–d) BALB/c mice were transplanted with TCD BM from B6.CD11c.GCDL mice (where luciferase is driven off the CD11c promoter) with or without B6.WT T cells, and BLI signals were quantified thereafter (to determine

Published July 13, 2015

of elimination by conditioning therapy and appear to have a very limited capacity to expand after BMT (Zhang et al., 2002), likely explaining the reported lack of effect of the DAMP/PAMP pathways in this compartment (Li et al., 2011). Moreover, such enhanced donor DC expansion and function in the GI tract may exacerbate not only acute but perhaps also chronic GVHD because it has been demonstrated that donor APCs play a dominant role in this setting (Anderson et al., 2005).

Donor $CD103^+CD11b^-$ DCs in the colon and the mLNs are the key players in indirect alloantigen presentation after BMT. Nonlymphoid tissue $CD103^+CD11b^-$ DCs correspond to the $CD8^+CD11b^-$ LN DCs and develop from pre-DC precursors but not monocytes at steady-state (Bogunovic et al., 2009; Varol et al., 2009). They are known to efficiently cross-present antigen and activate $CD8^+$ T cells (Shortman and Heath, 2010; Merad et al., 2013), but their ability to activate $CD4^+$ T cells is less clear. In addition, although inflammatory stimuli can increase DCs in the LNs, the origin of these inflammatory DCs remains unclear (Merad et al., 2013). Although monocytes had been considered progenitors (Auffray et al., 2009; Domínguez and Ardavín, 2010), hematopoietic stem cells have recently been described to give rise to $CD11c^+$ cells rapidly after LPS stimulation (Nagai et al., 2006; Massberg et al., 2007). We demonstrate that, like $CD8^+$ DCs in naive mice, the majority of donor $CD103^+CD11b^-$ DCs in the mLNs also express CD8 (Fig. S2). CCR2 controls monocyte recruitment from blood to inflamed tissue (Tsou et al., 2007), and we found that alloreactive T cell expansion was identical in recipients of CCR2-deficient and WT grafts (Fig. 5, b–f). Thus, the donor DCs essential for indirect alloantigen presentation in the mLNs would appear to be derived from the stem cell compartment rather than monocytes.

Consistent with previous studies (Maldonado-López et al., 1999; Fujimoto et al., 2011), $CD103^+CD11b^-$ DCs produce high amounts of IL-12p40 after BMT, and the absence of this cytokine reduced T cell expansion and Th1 cell differentiation. Notably, antigen presentation in isolation was not crucial for the generation of IFN-γ–producing donor T cells. Thus, MHC class II or CCR7-deficient donor DCs had minimal capacity to expand antigen-specific donor T cells and invoke Th17 cell differentiation, but some Th1 cell differentiation still occurred in this lymphopenic environment. However, it must be noted that the overall number of Th1 cells expanded in the absence of antigen presentation was very low. These findings are consistent with our previous observation that the complete absence of $I\text{-}A^b$ in BMT recipients did not completely prevent IFN-γ production by TEa cells (Koyama et al., 2012). However, in this setting the numbers generated are very low, they are not imprinted with α4β7, and they are unable to induce acute GVHD (Fig. 1 h; Koyama et al., 2012). Th17 cell differentiation required IL-6, and among DCs, this appeared to be predominantly derived from the $CD103^+CD11b^+$ subset. However, there is likely to be significant redundancy in the source of IL-6 after BMT because Th17 cell differentiation still occurred in recipients of $IRF4^{-/-}$ BM, which lack this population. Indeed, IL-6 is the principal dysregulated inflammatory cytokine after allogeneic BMT, and systemic levels are very high for 2 wk after BMT (Kennedy et al., 2014). Interestingly, we demonstrate that both IL-12 and IL-6 can expand alloreactive T cells within the gut independent of any effect on antigen presentation, providing an important rationale for their inhibition in the clinical setting. Indeed, we have recently demonstrated in a phase I/II study that the inhibition of IL-6 early after BMT is associated with very low levels of acute GVHD (Kennedy et al., 2014).

Surprisingly, antigen presentation by donor DCs exclusively controlled the expression of gut-homing integrins. Given that donor T cells cannot induce GVHD without alloantigen presentation (Koyama et al., 2012), these data demonstrate that Th1 T cells are insufficient to induce and/or maintain GVHD without the imprinting of gut tropism. As has been demonstrated for pathogens (Stagg et al., 2002; Johansson-Lindbom et al., 2005), we demonstrate that during GVHD this process is critically dependent on MHC class II presentation by donor DCs migrating from the colon. Together, these findings identify the hitherto unappreciated importance of indirect alloantigen presentation, amplified by GVHD, to the generation of lethal disease. We thus identify several molecular targets to prevent the development of severe GVHD in the clinic. These highlight first and foremost the importance in preventing GVHD and the feed-forward cascade thereafter that culminates in lethality. The cellular and molecular switches involved include the donor $CD103^+CD11b^-$ DC subset, IL-12, IL-6, DAMPs/PAMPs, and the RAGE pathway. Inhibition of the IL-6 receptor with tocilizumab, a humanized monoclonal antibody, has shown promise in reducing the incidence of acute GVHD, including intestinal GVHD, in a phase I/II clinical trial (Kennedy et al., 2014). Likewise, IL-12 blocking antibodies (ustekinumab) and RAGE inhibitors (FPS-ZM1) are now available (Henden and Hill, 2015). Therapeutic approaches inhibiting this amplification cascade within acute GVHD can thus now be tested in the clinic.

donor DC expansion). Experimental schema (a), representative BLI on days 3, 5, 12, and 21 (b), quantified BLI signals in colon, small intestine, and mLNs (c), and ratio of BLI signals from mice receiving BM and B6.WT T cells to those from mice receiving TCD BM alone on day 12 by mixed-model analysis (d). Time course shown in c is combined from three experiments (n = 3–9 per time point). Data on days 5, 8, 12, and 21 are combined from two replicate experiments. *, P = 0.0499, day 12 versus day 21 of BM + T in small intestine; ***, P = 0.002, day 12 versus day 21 of TCD BM in mLN; BM + T versus TCD BM ****, P < 0.0001 (day 21); ***, P = 0.0009 (day 12); **, P = 0.0093 (day 28) in colon; ****, P < 0.0001 (days 12 and 21) in small intestine; ***, P = 0.0006 (day 21); *, P = 0.0257 (day 28) in mLNs. (e) BALB/c mice were transplanted with TCD BM with or without T cells from B6.IL-12p40-YFP ($CD45.2^+$) mice. Representative FACS plots of the $CD3^-NKp46^-CD45.2^+$ fraction from the isolated colon, small intestine, and mLNs on day 12 are shown and are representative of two replicate experiments. Data are represented as mean ± SEM.

Published July 13, 2015

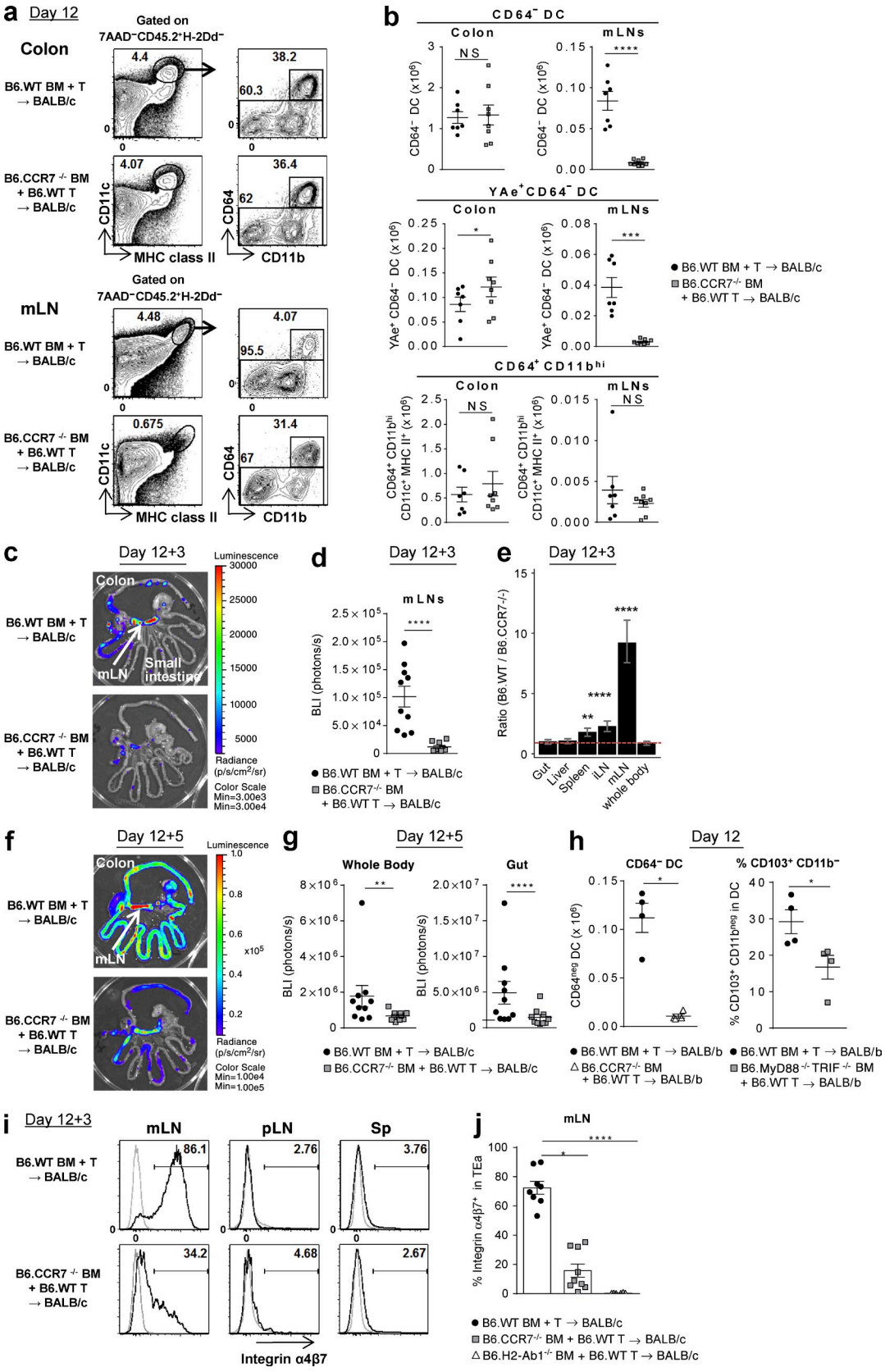

Figure 10. Colon-derived donor DCs migrate to the mLNs via CCR7 and imprint the α4β7 gut-homing integrin on donor T cells. (a–g, i, and j) BALB/c mice were transplanted with TCD BM from B6.WT, B6.CCR7$^{-/-}$, or B6.H2-Ab1$^{-/-}$ mice with B6.WT T cells. (a and b) Colon and mLNs were isolated

Published July 13, 2015

MATERIALS AND METHODS

Mice. BALB/b (H-2^b, CD45.2$^+$), C57BL/6 (B6.WT, H-2^b, CD45.2$^+$), C57BL/6 background Ptprc^a (B6.CD45.1$^+$, H-2^b, CD45.1$^+$), and BALB/c (H-2^d, CD45.2$^+$) were purchased from the Animal Resources Centre. Transgenic and knockout mice on a B6 background originated as follows: B6.IL-12p40YFP, C.R. Engwerda; BALB/c background Ptprc^a (BALB/c.CD45.1$^+$, H-2^d, CD45.1$^+$), B6.IL-12p40$^{-/-}$, and B6.CCR2$^{-/-}$, M.J. Smyth; B6.CD11c.ova and B6.OT-II, R. Steptoe, University of Queensland (UQ), St. Lucia, Queensland, Australia; HY-TCR, A. Strasser, Walter and Eliza Hall Institution (WEHI), Melbourne, Victoria, Australia (Bouillet et al., 2002); B6.H2-Ab1$^{-/-}$, referred to as MHC class II$^{-/-}$, Australian National University, Canberra; B6.CD11c.GCDL, G. Hammerling, Deutsches Krebsforschungszentrum, Molekulare Immunologie, Heidelberg, Germany (Tittel et al., 2012); β-actin–luciferase, R. Negrin, Stanford University, Stanford, CA (Nishimura et al., 2008); TEa, J. Bromberg, Albert Einstein College of Medicine, Bronx, NY (Ochando et al., 2006); B6.IRF4$^{-/-}$, G.T. Belz (Mittrücker et al., 1997; Cretney et al., 2011); B6.MyD88$^{-/-}$TRIF$^{-/-}$, S. Akira, Osaka University, Osaka, Japan (Yamamoto et al., 2003); B6.RAGE$^{-/-}$, S. Phipps, UQ (Chen et al., 2008); CCR7$^{-/-}$, S.R. McColl (Bunting et al., 2013); and B6.CSF1R$^{-/+}$, R. Stanley, Albert Einstein College of Medicine (Alexander et al., 2014). TEa transgenics were similarly bred onto β-actin–luciferase (TEa^{luc+}) and CD45.1$^+$ backgrounds. Mice were bred at the QIMR Berghofer Medical Research Institute animal facilities. Mice including donors and recipients were female except the experiments as described using HY-TCR transgenics. Mice were housed in sterilized microisolator cages and received acidified autoclaved water, pH 2.5, after transplantation. All animal maintenance and procedures were undertaken using protocols approved by the institutional (QIMR) animal ethics committee.

Stem cell transplantation and reporter cell injection. BALB/c and BALB/b mice were transplanted as described previously (Morris et al., 2005) after 900 cGy total body irradiation (TBI; ^{137}Cs source at 84 cGy/min) on day −1. On day 0, mice were transplanted with 10×10^6 BM cells from B6.WT or the indicated B6 background transgenic mice with or without 2×10^5 FACS-purified B6.WT T cells (>98%; CD90.2$^+$). BM cells were depleted of T cells (TCD) by antibody and complement as previously described (MacDonald et al., 2007). For reporter assays, recipients were injected intravenously on day 12 with 2×10^6 TEa T cells, 10^6 HY-TCR CD8 Tg T cells, or 2×10^6 OT-II T cells to report alloantigen presentation. TEa (>98%; Vβ6$^+$Vα2$^+$), HY-TCR CD8 Tg (>98%; CD4$^-$CD90.2$^+$), and OT-II (>98%; Vβ5$^+$Vα2$^+$) cells were purified by sorting (MoFlo [Beckman Coulter] or FACSAria [BD]) as described previously (Markey et al., 2010). CFSE labeling has been described previously (Reddy et al., 2001; Banovic et al., 2005). For donor DC depletion, mice received 100 ng DT intraperitoneally every 2 d from day 8 to the day before analysis. The degree of systemic GVHD was assessed by scoring as previously described (maximum index = 10; Hill et al., 1997). For survival experiments, transplanted mice were monitored daily, and those with GVHD clinical scores ≥6 were sacrificed and the date of death registered as the next day, in accordance with institutional guidelines.

BLI. TEa^{luc+} T cell expansion was analyzed by luciferase signal intensity (Xenogen IVIS 100; Caliper Life Sciences). Light emission is presented as photons per second per square centimeter per steer radiant (ph/s/cm^2/sr). Total flux of mouse or organ is presented as photons per second (ph/s). Mice were injected with 500 µg D-Luciferin (subcutaneously; PerkinElmer) and imaged 5 min later.

Cell isolation from small intestine and colon. Small intestine and colon were removed, cut longitudinally into 3–5-mm pieces, and washed three times with PBS. The pieces were incubated under stirring in Ca/Mg-free PBS containing 5 mM EDTA (Chem-Supply) for 30 min at 37°C. Cells were isolated by passing through a 100-µm cell strainer. Suspended cells were kept as the intraepithelial leukocyte (IEL) fraction. The remaining pieces of tissue were incubated for 30 min at 37°C in RPMI including 5 µg/ml DNase + 5 µg/ml Collagenase 4 (Sigma-Aldrich) and then passed through a 100-µm cell strainer to obtain the lamina propria leukocyte (LPL) fraction. IEL and LPL fractions were combined for FACS analysis. In some experiments using colon, longitudinally cut pieces were processed with Gentle MACS (Miltenyi Biotec) according to the manufacturer's protocol.

FACS analysis. FITC-conjugated antibodies to CD45.1, CD45.2, H-2D^d, MHC class II (I-A/I-E), and IgG2a isotype control; PE-conjugated antibodies to CD11c, CD103, I-A^b, IFN-γ, CD40, CD80, CD86, CD115, Armenian Hamster IgG, and rat IgG2a isotype controls; PerCPCy5.5-conjugated antibody to CD11b; Cy7 PE (PeCy7)–conjugated antibodies to CD45.1, CD3, NKp46, CD64, and rat IgG2b isotype controls; allophycocyanin-conjugated antibodies to CD45.2, CD3, NK1.1, CD11c, CD103, CCR7, rat IgG2a, and rat IgG2b isotype control; Alexa Fluor 647–conjugated H-2D^d, I-A^d, Foxp3, mouse IgG1, and rat IgG2b isotype controls; Alexa Fluor 700–conjugated antibodies to CD45.1, F4/80, IL-17A, rat IgG2a, and IgG2b isotype controls; allophycocyanin-Cy7–conjugated antibody to CD11c; and Pacific Blue–conjugated I-A/I-E, Brilliant Violet 605–conjugated streptavidin, and antibody to CD90.2 were purchased from BioLegend. FITC-conjugated or biotin-conjugated antibodies to Vβ6, PE, or allophycocyanin-Cy7–conjugated antibodies to Vα2, Alexa Fluor 647–conjugated antibody to CD64 (a and b), and Alexa Fluor 700–conjugated antibody to CD45.2 were purchased from BD. Biotinylated antibodies to YAe and mouse IgG1 were purchased from eBioscience. The YAe antibody reacts with Ea peptide (peptide 52–68) bound to I-A^b (the same complex recognized by TEa cells). Allophycocyanin-conjugated antibody to CCR2 was purchased from R&D Systems. FITC-conjugated rat IgG2b isotype control (MAC5) was made in our laboratory. LIVE/DEAD Fixable Aqua Dead Cell Stain kit from Thermo Fisher Scientific was used to exclude dead cells according to the manufacturer's protocol. Foxp3 expression level with IFN-γ and IL-17A was determined using the Foxp3 staining buffer set (eBioscience) according to the manufacturer's protocol.

Mixed lymphocyte cultures. Mixed lymphocyte cultures were set up in triplicate in round-bottom 96-well plates (Falcon; BD) using sort-purified TEa T cells stimulated with CD11c$^+$ DCs from BALB/c recipients transplanted with BM and T cell of B6.WT mice 12 d after BMT, which were positively selected using CD11c beads and the magnetically activated cell sorter (MACS) system (Miltenyi Biotec) as previously described (Markey et al., 2010). TEa proliferation was determined by [^{3}H]thymidine uptake.

on day 12. Representative FACS plots (a) and the absolute numbers of CD64$^-$ DC, YAe$^+$CD64$^-$ DC, and CD64$^+$CD11b^{hi} subsets (b). Data shown are combined from three replicate experiments (n = 7–8 per group). ****, P < 0.0001; ***, P = 0.0003; *, P = 0.0413. (c–g, i, and j) On day 12 TEa^{luc+} T cells were injected, and 3 (c–e, i, and j) or 5 d (f and g) later BLI signals and cells from spleen, mLNs, and pLNs were analyzed. Representative BLI (c and f) and quantification of BLI signals (d and g). ****, P < 0.0001; **, P = 0.0012. (e) Ratio of BLI signals from B6.WT BM recipients to those from B6.CCR7$^{-/-}$ BM recipients by mixed-model analysis. ****, P < 0.0001; **, P = 0.00301 versus whole body. Data shown are combined from two replicate experiments (n = 9–10 per group). (h) BALB/b (H-2^b) mice were transplanted with TCD BM from B6.WT, B6.CCR7$^{-/-}$, or B6.MyD88$^{-/-}$TRIF$^{-/-}$ mice with B6.WT T cells, and mLNs were isolated on day 12. The absolute numbers of CD64$^-$ DCs and the frequency of the CD103$^+$CD11b$^-$ DC subset are shown. Data shown (n = 4 per group) are representative of two replicate experiments. *, P = 0.0286 (CD64$^-$ DC); *, P = 0.0367 (% CD103$^+$CD11b$^-$). (i and j) Representative FACS plots (i) and quantification (j) for α4β7 integrin expression, gated on TEa cells. Data shown are combined from two replicate experiments (n = 6–9 per group). ****, P < 0.0001; *, P = 0.0198. Data are represented as mean ± SEM.

Cytokine analysis. For direct cytokine detection, cells were stimulated ex vivo by 50 ng/ml PMA and 500 ng/ml ionomycin for 4 h at 37°C, and 1 µg/ml brefeldin A was added for the last 3 h. After surface staining, cells were fixed and permeabilized using the eBioscience Foxp3 intracellular staining kit, followed by staining of Foxp3, IFN-γ, and IL-17A. For IL-12p40 staining, cells were incubated with GolgiPlug (1 in 1,000 dilution; BD) for 4 h, followed by intracellular cytokine staining using the Cytofix/Cytoperm kit as per the manufacturer's protocol (BD). For quantitative PCR analyses, total RNA was extracted with the RNeasy Micro kit (QIAGEN) from sort-purified (>95% purity) cells and gene expression determined using TaqMan gene expression assays (Applied Biosystems). All measurements were run in parallel with the housekeeping gene *hprt* as an endogenous control. Data were normalized to both endogenous control and splenic $CD103^+$ DC population.

Statistical analysis. The natural log of bioluminescence values was taken before analysis. All other measurements (percentages and cell counts) remained untransformed. When experiments were replicated on separate days, the results were combined and analyzed via a two-way ANOVA where the two factors were day and experimental group. If there were no replications on separate days, a one-way ANOVA was performed. However, an ANOVA was only performed if the equality of variance tests indicated the group variances were not significantly different ($P > 0.01$). Otherwise an appropriate nonparametric test was performed. The mean ± SEM for the raw data (calculated on the linear scale) is presented.

To assess the differences in the decrease (or increase) in log bioluminescence for the experiment group relative to the appropriate WT, a mixed-model with mouse as a random effect was fitted and the interaction of organ by group was tested. If significant, a post-hoc comparison was performed by defining a contrast matrix and calculating a standard error estimate as per Cochran and Cox (1957), and the degrees of freedom were similarly calculated. The mean ± SEM for the ratio of the WT group to the appropriate experimental group for each organ was calculated on the log scale using the weighted standard error estimate as detailed above and then back transformed for ease of interpretation. For survival data, Kaplan-Meier curves were compared using the log-rank test. Where applicable, all p-values were corrected for multiple comparisons using the Bonferroni correction.

Online supplemental material. Fig. S1 depicts the proposed feed-forward cascade of acute GVHD mediated by colon-derived donor DCs. Fig. S2 shows the gating strategy of DCs in naive and post-BMT recipients. Online supplemental material is available at http://www.jem.org/cgi/content/full/jem.20150329/DC1.

We thank Andreas Schlitzer (Singapore Immunology Network, Singapore) for intellectual input for gut digestion methods, Kerenaftali Klein for expert statistical analysis, Paula Hall, Michael Rist, and Grace Chojnowski for expert cell sorting, and the animal facilities of QIMR and Madeleine Flynn for expert graphical work.

This work was supported by research grants from the National Health and Medical Research Council (NHMRC). M. Koyama is a Leukaemia Foundation of Australia Postdoctoral Fellow. K.A. Markey and S.-K. Tey are NHMRC Clinical Training Fellows. M.W.L. Teng is an NHMRC Career Development Fellow. C.R. Engwerda is an NHMRC Senior Research Fellow. M.J. Smyth is an NHMRC Senior Principal Research Fellow. G.T. Belz is an Australian Research Council Future Fellow. K.P.A. MacDonald is a Cancer Council of Queensland Fellow. G.R. Hill is an NHMRC Australian Fellow and QLD Health Senior Clinical Research Fellow.

The authors declare no competing financial interests.

Author contributions: M. Koyama designed, performed, and analyzed all experiments and wrote the paper. M. Cheong, K.A. Markey, K.H. Gartlan, R.D. Kuns, K.R. Locke, K.E. Lineburg, B.E. Teal, L. Leveque-El mouttie, M.D. Bunting, S. Vuckovic, P. Zhang, M.W.L. Teng, A. Varelias, and S.-K. Tey performed research and helped design experiments. L.F. Wockner performed statistical analysis. C.R. Engwerda, M.J. Smyth, G.T. Belz, and S.R. McColl provided critical reagents and data interpretation. K.P.A. MacDonald designed research and helped write the paper. G.R. Hill designed research and wrote the paper.

Submitted: 23 February 2015
Accepted: 26 June 2015

REFERENCES

Alexander, K.A., R. Flynn, K.E. Lineburg, R.D. Kuns, B.E. Teal, S.D. Olver, M. Lor, N.C. Raffelt, M. Koyama, L. Leveque, et al. 2014. CSF-1–dependent donor-derived macrophages mediate chronic graft-versus-host disease. *J. Clin. Invest.* 124:4266–4280. http://dx.doi.org/10.1172/JCI75935

Anderson, B.E., J.M. McNiff, D. Jain, B.R. Blazar, W.D. Shlomchik, and M.J. Shlomchik. 2005. Distinct roles for donor- and host-derived antigen-presenting cells and costimulatory molecules in murine chronic graft-versus-host disease: requirements depend on target organ. *Blood.* 105:2227–2234. http://dx.doi.org/10.1182/blood-2004-08-3032

Auffray, C., M.H. Sieweke, and F. Geissmann. 2009. Blood monocytes: development, heterogeneity, and relationship with dendritic cells. *Annu. Rev. Immunol.* 27:669–692. http://dx.doi.org/10.1146/annurev.immunol.021908.132557

Banovic, T., K.P. MacDonald, E.S. Morris, V. Rowe, R. Kuns, A. Don, J. Kelly, S. Ledbetter, A.D. Clouston, and G.R. Hill. 2005. TGF-β in allogeneic stem cell transplantation: friend or foe? *Blood.* 106:2206–2214. http://dx.doi.org/10.1182/blood-2005-01-0062

Blazar, B.R., W.J. Murphy, and M. Abedi. 2012. Advances in graft-versus-host disease biology and therapy. *Nat. Rev. Immunol.* 12:443–458. http://dx.doi.org/10.1038/nri3212

Bogunovic, M., F. Ginhoux, J. Helft, L. Shang, D. Hashimoto, M. Greter, K. Liu, C. Jakubzick, M.A. Ingersoll, M. Leboeuf, et al. 2009. Origin of the lamina propria dendritic cell network. *Immunity.* 31:513–525. http://dx.doi.org/10.1016/j.immuni.2009.08.010

Bouillet, P., J.F. Purton, D.I. Godfrey, L.C. Zhang, L. Coultas, H. Puthalakath, M. Pellegrini, S. Cory, J.M. Adams, and A. Strasser. 2002. BH3-only Bcl-2 family member Bim is required for apoptosis of autoreactive thymocytes. *Nature.* 415:922–926. http://dx.doi.org/10.1038/415922a

Bunting, M.D., I. Comerford, N. Seach, M.V. Hammett, D.L. Asquith, H. Körner, R.L. Boyd, R.J. Nibbs, and S.R. McColl. 2013. CCX-CKR deficiency alters thymic stroma impairing thymocyte development and promoting autoimmunity. *Blood.* 121:118–128. http://dx.doi.org/10.1182/blood-2012-06-434886

Chakraverty, R., and M. Sykes. 2007. The role of antigen-presenting cells in triggering graft-versus-host disease and graft-versus-leukemia. *Blood.* 110:9–17. http://dx.doi.org/10.1182/blood-2006-12-022038

Chen, X., R. Das, R. Komorowski, A. Beres, M.J. Hessner, M. Mihara, and W.R. Drobyski. 2009. Blockade of interleukin-6 signaling augments regulatory T-cell reconstitution and attenuates the severity of graft-versus-host disease. *Blood.* 114:891–900. http://dx.doi.org/10.1182/blood-2009-01-197178

Chen, Y., E.M. Akirav, W. Chen, O. Henegariu, B. Moser, D. Desai, J.M. Shen, J.C. Webster, R.C. Andrews, A.M. Mjalli, et al. 2008. RAGE ligation affects T cell activation and controls T cell differentiation. *J. Immunol.* 181:4272–4278. http://dx.doi.org/10.4049/jimmunol.181.6.4272

Cochran, W.G., and G.M. Cox. 1957. Experimental Designs. Second edition. Wiley, New York. 617 pp.

Cooke, K.R., G.R. Hill, J.M. Crawford, D. Bungard, Y. Brinson, J. Delmonte, and J.L.M. Ferrara. 1998. Tumor necrosis factor-α production to lipopolysaccharide stimulation by donor cells predicts the severity of experimental acute graft-versus-host disease. *J. Clin. Invest.* 102:1882–1891. http://dx.doi.org/10.1172/JCI4285

Cretney, E., A. Xin, W. Shi, M. Minnich, F. Masson, M. Miasari, G.T. Belz, G.K. Smyth, M. Busslinger, S.L. Nutt, and A. Kallies. 2011. The transcription factors Blimp-1 and IRF4 jointly control the differentiation and function of effector regulatory T cells. *Nat. Immunol.* 12:304–311. http://dx.doi.org/10.1038/ni.2006

Domínguez, P.M., and C. Ardavín. 2010. Differentiation and function of mouse monocyte-derived dendritic cells in steady state and inflammation. *Immunol. Rev.* 234:90–104. http://dx.doi.org/10.1111/j.0105-2896.2009.00876.x

Ferrara, J.L., J.E. Levine, P. Reddy, and E. Holler. 2009. Graft-versus-host disease. *Lancet.* 373:1550–1561. http://dx.doi.org/10.1016/S0140-6736(09)60237-3

Fujimoto, K., T. Karuppuchamy, N. Takemura, M. Shimohigoshi, T. Machida, Y. Haseda, T. Aoshi, K.J. Ishii, S. Akira, and S. Uematsu. 2011. A new subset of CD103$^+$CD8α^+ dendritic cells in the small intestine expresses TLR3, TLR7, and TLR9 and induces Th1 response and CTL activity. *J. Immunol.* 186:6287–6295. http://dx.doi.org/10.4049/jimmunol.1004036

Gooley, T.A., J.W. Chien, S.A. Pergam, S. Hingorani, M.L. Sorror, M. Boeckh, P.J. Martin, B.M. Sandmaier, K.A. Marr, F.R. Appelbaum, et al. 2010. Reduced mortality after allogeneic hematopoietic-cell transplantation. *N. Engl. J. Med.* 363:2091–2101. http://dx.doi.org/10.1056/NEJMoa1004383

Hashimoto, D., A. Chow, M. Greter, Y. Saenger, W.H. Kwan, M. Leboeuf, F. Ginhoux, J.C. Ochando, Y. Kunisaki, N. van Rooijen, et al. 2011. Pretransplant CSF-1 therapy expands recipient macrophages and ameliorates GVHD after allogeneic hematopoietic cell transplantation. *J. Exp. Med.* 208:1069–1082. http://dx.doi.org/10.1084/jem.20101709

Heidegger, S., M.R. van den Brink, T. Haas, and H. Poeck. 2014. The role of pattern-recognition receptors in graft-versus-host disease and graft-versus-leukemia after allogeneic stem cell transplantation. *Front. Immunol.* 5:337. http://dx.doi.org/10.3389/fimmu.2014.00337

Henden, A.S., and G.R. Hill. 2015. Cytokines in Graft-versus-Host Disease. *J. Immunol.* 194:4604–4612. http://dx.doi.org/10.4049/jimmunol.1500117

Hill, G.R., J.M. Crawford, K.R. Cooke, Y.S. Brinson, L. Pan, and J.L.M. Ferrara. 1997. Total body irradiation and acute graft-versus-host disease: the role of gastrointestinal damage and inflammatory cytokines. *Blood.* 90:3204–3213.

Hirano, T. 1998. Interleukin 6 and its receptor: ten years later. *Int. Rev. Immunol.* 16:249–284. http://dx.doi.org/10.3109/08830189809042997

Joffre, O.P., E. Segura, A. Savina, and S. Amigorena. 2012. Cross-presentation by dendritic cells. *Nat. Rev. Immunol.* 12:557–569. http://dx.doi.org/10.1038/nri3254

Johansson-Lindbom, B., M. Svensson, O. Pabst, C. Palmqvist, G. Marquez, R. Förster, and W.W. Agace. 2005. Functional specialization of gut CD103$^+$ dendritic cells in the regulation of tissue-selective T cell homing. *J. Exp. Med.* 202:1063–1073. http://dx.doi.org/10.1084/jem.20051100

Kennedy, G.A., A. Varelias, S. Vuckovic, L. Le Texier, K.H. Gartlan, P. Zhang, G. Thomas, L. Anderson, G. Boyle, N. Cloonan, et al. 2014. Addition of interleukin-6 inhibition with tocilizumab to standard graft-versus-host disease prophylaxis after allogeneic stem-cell transplantation: a phase 1/2 trial. *Lancet Oncol.* 15:1451–1459. http://dx.doi.org/10.1016/S1470-2045(14)71017-4

Kondo, T., T. Kawai, and S. Akira. 2012. Dissecting negative regulation of Toll-like receptor signaling. *Trends Immunol.* 33:449–458. http://dx.doi.org/10.1016/j.it.2012.05.002

Koyama, M., R.D. Kuns, S.D. Olver, N.C. Raffelt, Y.A. Wilson, A.L. Don, K.E. Lineburg, M. Cheong, R.J. Robb, K.A. Markey, et al. 2012. Recipient nonhematopoietic antigen-presenting cells are sufficient to induce lethal acute graft-versus-host disease. *Nat. Med.* 18:135–142. http://dx.doi.org/10.1038/nm.2597

Li, H., C. Matte-Martone, H.S. Tan, S. Venkatesan, J. McNiff, A.J. Demetris, D. Jain, F. Lakkis, D. Rothstein, and W.D. Shlomchik. 2011. Graft-versus-host disease is independent of innate signaling pathways triggered by pathogens in host hematopoietic cells. *J. Immunol.* 186:230–241. http://dx.doi.org/10.4049/jimmunol.1002965

MacDonald, K.P., R.D. Kuns, V. Rowe, E.S. Morris, T. Banovic, H. Bofinger, B. O'Sullivan, K.A. Markey, A.L. Don, R. Thomas, and G.R. Hill. 2007. Effector and regulatory T-cell function is differentially regulated by RelB within antigen-presenting cells during GVHD. *Blood.* 109:5049–5057. http://dx.doi.org/10.1182/blood-2007-01-067249

MacDonald, K.P., J.S. Palmer, S. Cronau, E. Seppanen, S. Olver, N.C. Raffelt, R. Kuns, A.R. Pettit, A. Clouston, B. Wainwright, et al. 2010. An antibody against the colony-stimulating factor 1 receptor depletes the resident subset of monocytes and tissue- and tumor-associated macrophages but does not inhibit inflammation. *Blood.* 116:3955–3963. http://dx.doi.org/10.1182/blood-2010-02-266296

Maldonado-López, R., T. De Smedt, P. Michel, J. Godfroid, B. Pajak, C. Heirman, K. Thielemans, O. Leo, J. Urbain, and M. Moser. 1999. CD8α^+ and CD8α^- subclasses of dendritic cells direct the development of distinct T helper cells in vivo. *J. Exp. Med.* 189:587–592. http://dx.doi.org/10.1084/jem.189.3.587

Markey, K.A., T. Banovic, R.D. Kuns, S.D. Olver, A.L. Don, N.C. Raffelt, Y.A. Wilson, L.J. Raggatt, A.R. Pettit, J.S. Bromberg, et al. 2009. Conventional dendritic cells are the critical donor APC presenting alloantigen after experimental bone marrow transplantation. *Blood.* 113:5644–5649. http://dx.doi.org/10.1182/blood-2008-12-191833

Markey, K.A., A.C. Burman, T. Banovic, R.D. Kuns, N.C. Raffelt, V. Rowe, S.D. Olver, A.L. Don, E.S. Morris, A.R. Pettit, et al. 2010. Soluble lymphotoxin is an important effector molecule in GVHD and GVL. *Blood.* 115:122–132. http://dx.doi.org/10.1182/blood-2009-01-199927

Markey, K.A., M. Koyama, R.D. Kuns, K.E. Lineburg, Y.A. Wilson, S.D. Olver, N.C. Raffelt, A.L. Don, A. Varelias, R.J. Robb, et al. 2012. Immune insufficiency during GVHD is due to defective antigen presentation within dendritic cell subsets. *Blood.* 119:5918–5930. http://dx.doi.org/10.1182/blood-2011-12-398164

Markey, K.A., K.P. MacDonald, and G.R. Hill. 2014. The biology of graft-versus-host disease: experimental systems instructing clinical practice. *Blood.* 124:354–362. http://dx.doi.org/10.1182/blood-2014-02-514745

Massberg, S., P. Schaerli, I. Knezevic-Maramica, M. Köllnberger, N. Tubo, E.A. Moseman, I.V. Huff, T. Junt, A.J. Wagers, I.B. Mazo, and U.H. von Andrian. 2007. Immunosurveillance by hematopoietic progenitor cells trafficking through blood, lymph, and peripheral tissues. *Cell.* 131:994–1008. http://dx.doi.org/10.1016/j.cell.2007.09.047

Matte, C.C., J. Liu, J. Cormier, B.E. Anderson, I. Athanasiadis, D. Jain, J. McNiff, and W.D. Shlomchik. 2004. Donor APCs are required for maximal GVHD but not for GVL. *Nat. Med.* 10:987–992. http://dx.doi.org/10.1038/nm1089

Merad, M., P. Sathe, J. Helft, J. Miller, and A. Mortha. 2013. The dendritic cell lineage: ontogeny and function of dendritic cells and their subsets in the steady state and the inflamed setting. *Annu. Rev. Immunol.* 31:563–604. http://dx.doi.org/10.1146/annurev-immunol-020711-074950

Mittrücker, H.W., T. Matsuyama, A. Grossman, T.M. Kündig, J. Potter, A. Shahinian, A. Wakeham, B. Patterson, P.S. Ohashi, and T.W. Mak. 1997. Requirement for the transcription factor LSIRF/IRF4 for mature B and T lymphocyte function. *Science.* 275:540–543. http://dx.doi.org/10.1126/science.275.5299.540

Morris, E.S., K.P. MacDonald, V. Rowe, T. Banovic, R.D. Kuns, A.L. Don, H.M. Bofinger, A.C. Burman, S.D. Olver, N. Kienzle, et al. 2005. NKT cell-dependent leukemia eradication following stem cell mobilization with potent G-CSF analogs. *J. Clin. Invest.* 115:3093–3103. http://dx.doi.org/10.1172/JCI25249

Nagai, Y., K.P. Garrett, S. Ohta, U. Bahrun, T. Kouro, S. Akira, K. Takatsu, and P.W. Kincade. 2006. Toll-like receptors on hematopoietic progenitor cells stimulate innate immune system replenishment. *Immunity.* 24:801–812. http://dx.doi.org/10.1016/j.immuni.2006.04.008

Nishimura, R., J. Baker, A. Beilhack, R. Zeiser, J.A. Olson, E.I. Sega, M. Karimi, and R.S. Negrin. 2008. In vivo trafficking and survival of cytokine-induced killer cells resulting in minimal GVHD with retention of antitumor activity. *Blood.* 112:2563–2574. http://dx.doi.org/10.1182/blood-2007-06-092817

Ochando, J.C., C. Homma, Y. Yang, A. Hidalgo, A. Garin, F. Tacke, V. Angeli, Y. Li, P. Boros, Y. Ding, et al. 2006. Alloantigen-presenting plasmacytoid dendritic cells mediate tolerance to vascularized grafts. *Nat. Immunol.* 7:652–662. http://dx.doi.org/10.1038/ni1333

Persson, E.K., H. Uronen-Hansson, M. Semmrich, A. Rivollier, K. Hägerbrand, J. Marsal, S. Gudjonsson, U. Håkansson, B. Reizis, K. Kotarsky, and W.W. Agace. 2013. IRF4 transcription-factor-dependent CD103$^+$ CD11b$^+$ dendritic cells drive mucosal T helper 17 cell differentiation. *Immunity.* 38:958–969. http://dx.doi.org/10.1016/j.immuni.2013.03.009

Reddy, P., T. Teshima, M. Kukuruga, R. Ordemann, C. Liu, K. Lowler, and J.L. Ferrara. 2001. Interleukin-18 regulates acute graft-versus-host disease by enhancing Fas-mediated donor T cell apoptosis. *J. Exp. Med.* 194:1433–1440. http://dx.doi.org/10.1084/jem.194.10.1433

Saleh, M., and G. Trinchieri. 2011. Innate immune mechanisms of colitis and colitis-associated colorectal cancer. *Nat. Rev. Immunol.* 11:9–20. http://dx.doi.org/10.1038/nri2891

Schlitzer, A., N. McGovern, P. Teo, T. Zelante, K. Atarashi, D. Low, A.W. Ho, P. See, A. Shin, P.S. Wasan, et al. 2013. IRF4 transcription

factor-dependent CD11b+ dendritic cells in human and mouse control mucosal IL-17 cytokine responses. *Immunity*. 38:970–983. http://dx.doi.org/10.1016/j.immuni.2013.04.011

Shlomchik, W.D., M.S. Couzens, C.B. Tang, J. McNiff, M.E. Robert, J. Liu, M.J. Shlomchik, and S.G. Emerson. 1999. Prevention of graft versus host disease by inactivation of host antigen-presenting cells. *Science*. 285:412–415. http://dx.doi.org/10.1126/science.285.5426.412

Shortman, K., and W.R. Heath. 2010. The $CD8^+$ dendritic cell subset. *Immunol. Rev.* 234:18–31. http://dx.doi.org/10.1111/j.0105-2896.2009.00870.x

Stagg, A.J., M.A. Kamm, and S.C. Knight. 2002. Intestinal dendritic cells increase T cell expression of $\alpha4\beta7$ integrin. *Eur. J. Immunol*. 32:1445–1454. http://dx.doi.org/10.1002/1521-4141(200205)32:5<1445::AID-IMMU1445>3.0.CO;2-E

Tamoutounour, S., S. Henri, H. Lelouard, B. de Bovis, C. de Haar, C.J. van der Woude, A.M. Woltman, Y. Reyal, D. Bonnet, D. Sichien, et al. 2012. CD64 distinguishes macrophages from dendritic cells in the gut and reveals the Th1-inducing role of mesenteric lymph node macrophages during colitis. *Eur. J. Immunol*. 42:3150–3166. http://dx.doi.org/10.1002/eji.201242847

Tawara, I., M. Koyama, C. Liu, T. Toubai, D. Thomas, R. Evers, P. Chockley, E. Nieves, Y. Sun, K.P. Lowler, et al. 2011. Interleukin-6 modulates graft-versus-host responses after experimental allogeneic bone marrow transplantation. *Clin. Cancer Res.* 17:77–88. http://dx.doi.org/10.1158/1078-0432.CCR-10-1198

Teshima, T., R. Ordemann, P. Reddy, S. Gagin, C. Liu, K.R. Cooke, and J.L. Ferrara. 2002. Acute graft-versus-host disease does not require alloantigen expression on host epithelium. *Nat. Med*. 8:575–581. http://dx.doi.org/10.1038/nm0602-575

Tittel, A.P., C. Heuser, C. Ohliger, C. Llanto, S. Yona, G.J. Hämmerling, D.R. Engel, N. Garbi, and C. Kurts. 2012. Functionally relevant neutrophilia in CD11c diphtheria toxin receptor transgenic mice. *Nat. Methods*. 9:385–390. http://dx.doi.org/10.1038/nmeth.1905

Toubai, T., I. Tawara, Y. Sun, C. Liu, E. Nieves, R. Evers, T. Friedman, R. Korngold, and P. Reddy. 2012. Induction of acute GVHD by sex-mismatched H-Y antigens in the absence of functional radiosensitive host hematopoietic-derived antigen-presenting cells. *Blood*. 119:3844–3853. http://dx.doi.org/10.1182/blood-2011-10-384057

Tsou, C.L., W. Peters, Y. Si, S. Slaymaker, A.M. Aslanian, S.P. Weisberg, M. Mack, and I.F. Charo. 2007. Critical roles for CCR2 and MCP-3 in monocyte mobilization from bone marrow and recruitment to inflammatory sites. *J. Clin. Invest*. 117:902–909. http://dx.doi.org/10.1172/JCI29919

Varelias, A., K.H. Gartlan, E. Kreijveld, S.D. Olver, M. Lor, R.D. Kuns, K.E. Lineburg, B.E. Teal, N.C. Raffelt, M. Cheong, et al. 2015. Lung parenchyma-derived IL-6 promotes IL-17A-dependent acute lung injury after allogeneic stem cell transplantation. *Blood*. 125:2435–2444. http://dx.doi.org/10.1182/blood-2014-07-590232

Varol, C., A. Vallon-Eberhard, E. Elinav, T. Aychek, Y. Shapira, H. Luche, H.J. Fehling, W.D. Hardt, G. Shakhar, and S. Jung. 2009. Intestinal lamina propria dendritic cell subsets have different origin and functions. *Immunity*. 31:502–512. http://dx.doi.org/10.1016/j.immuni.2009.06.025

Weisdorf, D., M.J. Zhang, M. Arora, M.M. Horowitz, J.D. Rizzo, and M. Eapen. 2012. Graft-versus-host disease induced graft-versus-leukemia effect: greater impact on relapse and disease-free survival after reduced intensity conditioning. *Biol. Blood Marrow Transplant*. 18:1727–1733. http://dx.doi.org/10.1016/j.bbmt.2012.06.014

Yamamoto, M., S. Sato, H. Hemmi, K. Hoshino, T. Kaisho, H. Sanjo, O. Takeuchi, M. Sugiyama, M. Okabe, K. Takeda, and S. Akira. 2003. Role of adaptor TRIF in the MyD88-independent toll-like receptor signaling pathway. *Science*. 301:640–643. http://dx.doi.org/10.1126/science.1087262

Zhang, Y., J.P. Louboutin, J. Zhu, A.J. Rivera, and S.G. Emerson. 2002. Preterminal host dendritic cells in irradiated mice prime CD8+ T cell-mediated acute graft-versus-host disease. *J. Clin. Invest*. 109:1335–1344. http://dx.doi.org/10.1172/JCI0214989